Climate Dynamics (2019) 53:1991–2011
https://doi.org/10.1007/s00382-019-04759-4

Improved climatological precipitation characteristics over West Africa at convection-permitting scales

Ségolène Berthou[1] · David P. Rowell[1] · Elizabeth J. Kendon[1] · Malcolm J. Roberts[1] · Rachel A. Stratton[2] · Julia A. Crook[3] · Catherine Wilcox[4]

Received: 8 June 2018 / Accepted: 5 April 2019 / Published online: 12 April 2019

Abstract
The West African climate is unique and challenging to reproduce using standard resolution climate models as a large proportion of precipitation comes from organised deep convection. For the first time, a regional 4.5 km convection permitting simulation was performed on a pan-African domain for a period of 10 years (1997–2006). The 4.5 km simulation (CP4A) is compared with a 25 × 40 km convection-parameterised model (R25) over West Africa. CP4A shows increased mean precipitation, which results in improvements in the mature phase of the West African monsoon but deterioration in the early and late phases. The distribution of precipitation rates is improved due to more short lasting intense rainfall events linked with mesoscale convective systems. Consequently, the CP4A model shows a better representation of wet and dry spells both at the daily and sub-daily time-scales. The diurnal cycle of rainfall is improved, which impacts the diurnal cycle of monsoon winds and increases moisture convergence in the Sahel. Although shortcomings were identified, with implications for model development, this convection-permitting model provides a much more reliable precipitation distribution than its convection-parameterised counterpart at both daily and sub-daily time-scales. Convection-permitting scales will therefore be useful to address the crucial question of how the precipitation distribution will change in the future.

1 Introduction

West-Africa is one of the most vulnerable areas in the world in terms of food security. It has a high sensitivity to climate risk (e.g. relying on rainfed agriculture) and little adaptive capacity (e.g. lack of infrastructure and a large proportion of the population below the poverty line) (Krishnamurthy et al. 2014). Changes in the magnitude and duration of climate hazards in this region can therefore have large effects on food security (Richardson et al. 2018), infrastructure, health and livelihoods. However, climate information at the required space and time scales is not yet reliably available for some high-impact events such as short lasting intense rainfall (Maraun et al. 2010).

The West African climate is dominated by a monsoonal system forced by the strong temperature gradient between the warm Sahara (Saharan Heat Low—SHL) and the colder waters of the Gulf of Guinea in boreal summer (Fontaine and Philippon 2000). The subsequent low level southwesterlies bring moist air inland and converge with the dry northeasterly Harmattan winds at the intertropical discontinuity (ITD), south of which most rainfall occurs. In April, rainfall is most frequent south of 10°N and by mid-June, the oceanic phase fades and the majority of rainfall shifts to the Soudanian zone (9°–12.5°N, annual rainfall amount exceeding 750 mm) until September. The Sahelian zone (12.5–18N, annual rainfall amount below 750 mm) receives most rainfall from June to September (Fink et al. 2017). The Guinea coast to the east of Cape Palmas has two rainy seasons: May–June and October, with a little dry season in July–August, during which small diurnal MCSs are dominant (Fiolleau and Roca 2013). The Soudano-Sahelian zone is unique as 75% (Soudanian zone) to 90% (Sahelian zone) of its rainfall results from fast-moving Mesoscale convective systems (MCSs) (Mathon et al. 2002; Fink et al. 2006), favoured by the combination of

✉ Ségolène Berthou
segolene.berthou@metoffice.gov.uk

1 Hadley Centre, Met Office, FitzRoy Rd, Exeter, UK

2 Met Office, FitzRoy Rd, Exeter, UK

3 School of Earth and Environment, University of Leeds, Leeds, UK

4 Institut des Géosciences de l'Environnement (IGE), Université Grenoble Alpes, Grenoble, France

large values of convective available potential energy (CAPE) and precipitable water (PW), mid-level dryness and vertical shear. The African easterly jet (AEJ) arising from the north–south low-level thermal gradient is largely responsible for the last two factors as it is maximum above this zone between 500 and 700 hPa and squall-line MCSs are often linked with African easterly waves (AEW).

Convection-parameterised models can reproduce some larger-scale MCSs at 25 km resolution (Vellinga et al. 2015) but km-scale convection-permitting models (CPMs) where the convection is explicitly represented are much more successful in representing them already at 12 km resolution in West Africa (Marsham et al. 2013; Birch et al. 2014; Maurer et al. 2017). These models are increasingly being used at climate and continental scales but so far their use has mainly focused on mid-latitude regions (Liu et al. 2016; Leutwyler et al. 2017; Berthou et al. 2018). In the framework of the Future Climate For Africa (FCFA) programme, a first-of-its-kind 10 year-long pan African convection-permitting simulation was run by the Met Office. Stratton et al. (2018) provided a detailed description of the simulation set-up and a first pan-African validation of the first 5 years of simulation. They showed a reduced dry bias over the Sahel in JJA and an associated reduction in short-wave radiative biases resulting from the presence of brighter, more organized convective clouds. Using TRMM as reference dataset, they showed that there is evidence of westward-propagating convective systems in the convection-permitting simulation and of better distribution of 3-hourly precipitation events in West-Africa. The most extreme intense but short-lived rainfall events are also better captured. The diurnal cycle of convective precipitation over land is better handled, although there is still a tendency for rain to initiate too early in the day.

The regional African Monsoon Multidisciplinary Analysis (AMMA-2050) project was set to improve understanding of climate change for the West African monsoon 5–40 years ahead to plan climate-resilient development. In this framework, we aim at informing the extent to which convection-permitting models can add value in West-Africa compared to convection-parameterised models for users of climate information related to rainfall, and document where further model development is needed. Section 2 first establishes the current state of CP-modeling over West Africa. In Sect. 3, the simulation set-up, the observational datasets and the methods are presented. Section 4 provides an overview of the changes brought by CP4A in the West African monsoon progression in terms of precipitation characteristics and propose some explanations of the differences with convection-parameterised simulation in the light of current knowledge. Acknowledging the large spatial and temporal variability of precipitation, Sect. 5 presents mean state maps in the peak monsoon season and Sect. 6 add details to the broader analysis of Stratton et al. (2018). In that section, we also provide a discussion about observational uncertainty thanks to comparisons with fine-resolution datasets and give an evaluation of precipitation at the model grid-scale in local sites. Finally, Sect. 7 shows the spatial distribution of the diurnal cycle of precipitation.

2 Background

The use of explicit convection in West-Africa in season-long simulations has shown the better representation of convective processes, which can then feed back onto improvements in the mean state of the monsoon. The main results from these previous studies are summarised here.

With case studies or season-long simulations, it was shown that Sahel MCSs are more likely to initiate by heating over the elevated terrain environments (Laing et al. 2012) or over convergent boundaries, such as those produced by land-surface vegetation or moisture anomalies, gust fronts and cold pool outflow or the diurnal migration of the inter-tropical discontinuity (ITD) (Taylor et al. 2013; Birch et al. 2014; Hartley et al. 2016; Maurer et al. 2017; Vizy and Cook 2018a). They also showed better coupling between AEWs and MCSs compared to convection-parameterised models (Birch et al. 2014; Vizy and Cook 2018a) and good representation of MCS lifecycles (Vizy and Cook 2018a).

Pearson et al. (2010a, 2014) also showed that explicit convection leads to an improved representation of the diurnal cycle of cloudiness and outgoing longwave radiation while Stein et al. (2015b) showed its influence on the vertical structure of clouds.

Furthermore, the better representation of cold pools leads to increased northward advection of cooler air into the Sahara (Pearson et al. 2010a; Marsham et al. 2011, 2013). The lack of cold pools in convection-parameterised models has been shown to significantly contribute to large-scale systematic biases in temperature and humidity observed over the central Sahara (Garcia-Carreras et al. 2013). The use of off-line dust models also showed that cold pools cause around 50% of summertime dust uplift in models with explicit convection, which is missing in models with parameterized convection (Marsham et al. 2011; Heinold et al. 2013).

The spatial complexity of the diurnal cycle has also been studied with convection-permitting models. Indeed, Zhang et al. (2016a) identified single peaks in the diurnal cycle of precipitation in observations occuring either in the afternoon or at night in different regions, highlighting the strong spatial gradients in the timing of the diurnal cycle. Zhang et al. (2016b) reproduced these single peaks with a convection-permitting model in August 2006 and concluded that afternoon rainfall peaks are associated with an unstable atmosphere, and that nocturnal rainfall peaks are associated with the westward

propagation of rainfall systems, as documented by Laing et al. (2008). However, their model tended to have too widespread night peaks away from the orography, which they related to too high boundary layer which prevented the triggering of afternoon convection. With the help of a 1 month-long simulation, Vizy and Cook (2018a) showed that nocturnal convection is not only due to afternoon orographic triggering in neighbouring regions, but also to more complex interactions between the Sahel ITD and atmospheric synoptic conditions over gradual-sloping terrain. Thanks to 3-month long simulations, Vizy and Cook (2018b) also shed light on the mechanisms at the origin of daytime convection away from the orography in two different regions: one closer to the direct influence of the monsoon flow (Burkina Faso) and one further away (eastern Niger/Nigeria). They showed different mechanisms in both regions. In Burkina Faso, daytime convection is a complex mix between long-lived convection triggered in the afternoon farther upstream and locally triggered convection at the left front exit of an easterly mid-level jet streak. In eastern Niger/Nigeria, daytime convection is mostly locally triggered and depends on whether the moist monsoon flow reaches the region, which is favoured by previous convection in upstream regions and the presence of an AEW disturbance.

This better representation of convective systems does have an impact on the mean state. In fact, Marsham et al. (2013); Birch et al. (2014) showed that the better diurnal cycle of convection in the Sahel in August led to changes in the diurnal cycle of winds through enhanced pressure gradients at night between the coast and the Sahel, and reduced pressure gradients between the Sahel and the Sahara, leading to stronger moisture convergence in the Sahel in convection-permitting models. This allowed the monsoon to be stronger and positioned further north in convection-permitting models. It turned the Sahel from being a moisture source in parameterised models (Meynadier et al. 2010b) to a more realistic moisture sink in an explicit model (Birch et al. 2014; Meynadier et al. 2010a).

These studies suggest that the precipitation distribution on longer time-scales in West Africa will be altered in convection-permitting models compared to convection-parameterised models, with implications for calculating user-relevant indices, usually derived from convection-parameterised models. They also point to changes in the mean state of the monsoon peak season and call for examination of the spatial complexity of the diurnal cycle in West Africa. We investigate these points in the present study thanks to a 10-year long convection-permitting simulation.

3 Simulations, observations and methods

3.1 Simulations

A brief summary of the simulation set-up is given here. A detailed description is available in Stratton et al. (2018).

We compare two 10-year long (1997–2006) regional climate simulations using the Met Office Unified Model (UM) (Walters et al. 2017) over a pan-African domain (45S–39N; 24W–56E):

- CP4A—a convection-permitting model at 4.5×4.5 km at the equator ($0.0405° \times 0.0405°$). In the absence of a scale-aware convection scheme, it does not include any convection parametrization and relies on the model dynamics to explicitly represent convective clouds.
- R25—a convection-parameterised model at 26×39 km resolution at the equator ($0.234° \times 0.351°$)

Both regional models are forced at their boundaries by a global model with the same resolution as R25 forced with 0.25° present-day daily sea surface temperature (SST) (Reynolds et al. 2007). The soil properties are those of sand in the whole continent in both simulations following De Kauwe et al. (2013) who found that the soil standard database used in the UM contains unrealistic small-scale variability across Africa. Both models also have the same aerosol climatology.

The regional R25 simulation was run with a near-identical set-up to CP4A. The remaining differences in model set-up are primarily because some hypotheses are not valid at km-scales: R25 has a one dimensional boundary layer scheme (Lock 2001) while CP4A has a three dimensional boundary-layer scheme (Boutle et al. 2014) with stochastic perturbations to temperature and moisture applied in the subcloud layer of cumulus-capped convective boundary layers. Another difference is the use of the a prognostic cloud fraction and condensation scheme [PC2; Wilson et al. (2008)] in R25 whereas CP4-Africa, like other convection-permitting UM formulations, uses the diagnostic Smith (1990) scheme. Finally, a moisture conservation scheme (Aranami et al. 2015) was implemented in CP4A but not in R25, partly because these errors are supposedly larger in convection-permitting models. This has the effect to reduce unrealistically strong precipitation intensities due to transport errors from the semi-lagrangian scheme. It also reduces mean precipitation in a spatially homogeneous way. More details can be found in Stratton et al. (2018).

The use of different cloud schemes may also influence some of our results but the Cascade studies (Pearson et al. 2010b, 2014; Birch et al. 2014) did not have differences

in the cloud scheme between their convection-parameterised models and convection-permitting model, and found qualitatively similar results as this study, so we believe that most of the changes between R25 and CP4A are due to switching convection off and increasing the resolution.

3.2 Observations

We use several high-resolution precipitation observational estimates to evaluate model performance, since each type of estimate has its advantages and drawbacks (Gehne et al. 2016). We use two high-resolution satellite retrievals: TRMM-3B42v7: Tropical Rainfall Measuring Mission (TRMM) (2011) and the gauge-corrected version of CMORPH (Xie et al. 2017). We also use 3 rain-gauge based precipitation estimates at mesosites in Niger, Mali and Benin from the African Monsoon Multi-disciplinary Analysis, Couplage de l'Atmosphère Tropicale et du Cycle Hydrologique (AMMA-CATCH).

Both satellite retrievals use high-resolution infrared brightness (IR) temperatures from geostationary satellites related to precipitation rates using the more accurate passive microwave (PMW) estimates from the polar-orbiting satellites. They differ by how the IR is calibrated, how PMW and IR measurements are related and by which bias correction is applied.

CMORPHv1-CRT In this dataset, high-quality PMW rainfall estimates are propagated by motion vectors derived from high-frequency IR imagery (Joyce et al. 2004). CMORPH is bias corrected against the gauge-based National Centers for Environmental Prediction (NCEP) Climate Prediction Center (CPC) daily precipitation analysis over land (Xie et al. 2010) and GPCP pentad data over the ocean. Correction over land is done by matching probability density functions against daily gauge analysis using optimal interpolation with orographic correction. CMORPH resolution is 8 km × 8 km and 30 mn, but we aggregated it on a 0.25 grid and 3-hourly to be comparable with TRMM and R25. We use 10 years (1998–2007) in the present study.

TRMM-3B42v7 In the Tropical Rainfall Measuring Mission 3B42v7 (TRMM), the monthly means of the 3-hourly microwave-calibrated IR rainfall estimates are combined with the GPCC monthly rain gauge analysis (Schneider et al. 2014) to generate a monthly satellite gauge combination (TRMM3B43). Each 3-hourly field is then scaled to sum to the corresponding monthly satellite gauge field (Tropical Rainfall Measuring Mission (TRMM) 2011). The dataset is 3-hourly and on a 0.25° grid. We use 10 years (1998–2007) in the present study.

AMMA-CATCH Three so-called mesosites with enhanced surface measurements were set up within the AMMA project: the Ouémé mesosite in central Benin (AMMA-CATCH 1996), the Niamey mesosite in southern Niger (AMMA-CATCH 1990) and the Gourma mesosite in Mali (AMMA-CATCH 2003). Within these three sites rain gauge networks are maintained by the Institut de Recherche pour le Développement (IRD) funded AMMA-CATCH program. Rainfall data at high temporal resolution are freely available from the AMMA-CATCH database (see http://www.amma-catch.org; data accessed in March 2018). In this study, we use the gridded versions of the datasets on a 4 km grid spanning 1999–2008 in Benin, 2006–2011 in Mali and 1997–2006 in Niger. They were derived from the rain-gauges by a dynamic interpolation method (Vischel et al. 2011). Their locations are shown in Fig. 1.

CHIRPS,CRU,ARC2 Three other datasets are used to compare their precipitation climatology. Two of them include both infrared imagery and stations: the Climate Hazards Group InfraRed Precipitation with Stations (CHIRPS) dataset (Funk et al. 2015a) and the Africa Rainfall

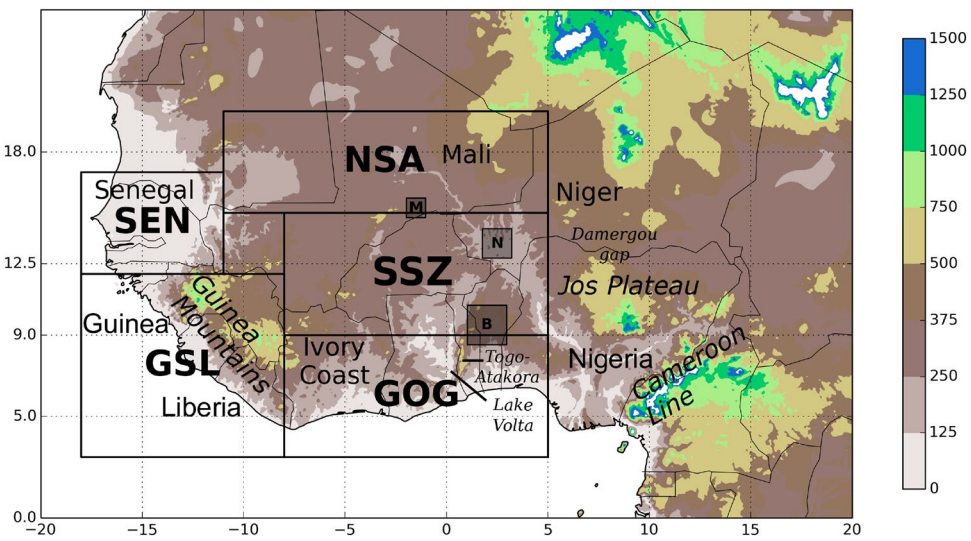

Fig. 1 CP4A orography (colour shading), definition of the zones used throughout the article and location of the three AMMA-CATCH meso-sites used in this study (M: Gourma, Mali, B: Ouémé, Benin, N: Niamey, Niger)

Climatology (ARC2) (Novella and Thiaw 2013). The third one is the station-based Climate Research Unit CRU TS-3.22 (Harris et al. 2014).

Dataset comparison CMORPH and to a lesser extent ARC2 have a very low precipitation intensity in Guinea, Sierra Leone and Liberia, in clear disagreement with all other datasets in this zone (Fig. 7). The low precipitation intensity in this new version of CMORPH comes from the bias correction against the NCEP-CPC rain-gauge analysis (Xie et al. 2017), which is clearly very different from GPCC (against which TRMM is corrected). ARC2 and CPC are using rain-gauges from the GTS network while GPCC, CHIRPS and CRU have extra sources of data including national datasets. ARC2 documentation reports that GTS stations in Gambia, Guinea-Bissau, Guinea, Sierra Leone, and Nigeria reported under 30% of the time from 1983 to 2009 (Novella and Thiaw 2013). Therefore, the constraint from gauges is weak in ARC2 and CMORPH. Although the station coverage is also quite low in the GSL region from year 2000 in GPCC, it relies on a climatology from earlier years (Schneider et al. 2014). We will therefore consider TRMM as more reliable in these regions. Note however that in other regions, we found that CMORPH had better rainfall intensities than TRMM (Sect. 6.1.2), so we chose it as reference dataset in most figures.

3.3 Methods

In Sect. 7.2, a precipitation object tracking algorithm is applied to CP4A and CMORPHv1-CRT following (Stein et al. 2015a). Both datasets are first regridded to a 12 km grid and the tracking is then applied to CMORPH 30 mn fields and CP4A 15 mn fields. At each time step clusters are identified as contiguous grid cells meeting a 1 mm/h threshold. A storm is then defined as clusters that propagate over a number of time steps, using an overlap criteria of 0.6 once the cluster is propagated using its estimated velocity. Clusters larger than 1000 km^2 are considered to be mesoscale convective systems whereas clusters smaller than 1000 km^2 are classified as small storms. R25 is not used since most clusters would be classed as MCSs due to its relatively coarse grid. Only four seasons were used since the algorithm is expensive to run on such high resolution fields: JAS 1999, 2000, 2001, 2004 for CP4A and 2001, 2002, 2004 and 2006 for CMORPH. Although the chosen years are different in CP4A and CMORPH partly due to the quality of CMORPH during those years, we believe this does not affect our results, as shown later by plotting different years separately.

For most of our analysis, CP4A, R25 and CMORPH are conservatively regridded to TRMM grid (0.25°) to ensure a fair comparison, as advised by Chen and Dai (2018). CP4A is only analysed on its native grid in Sect. 6.2 when compared to AMMA-CATCH observations and on a 12 km grid for the storm tracking.

The map diagnostics include stipplings where the difference between the model and the dataset is significantly different from year-to-year variability at the 5% global significance level. We used the following bootstrap method:

- Estimate local p value at individual grid points:
  1. The 10 years are re-sampled a 1000 times with replacement and the metric is calculated for each sample (same re-sampling for all datasets and models).
  2. The mean of the bootstrapped metric was computed, and subtracted from each bootstrap estimate; this creates a 1000 number of zero-centred metrics and gives us an estimate of the probability distribution of the test statistic under the null hypothesis.
  3. The original metric is then compared with this null distribution, and the p value is estimated based on which quantile the original metric corresponds to relative to the null distribution. For instance, if the original metric is below 2% or above 98% of the values in the simulated null distribution, the uncorrected p value would be 0.02.
- When carrying out field significance tests for map plots, one would expect some significant results to occur by chance (Wilks 2016). The problem is further complicated by the natural spatial correlation of geophysical data, which leads to incorrect identification of significant results. To address this problem we apply a correction to the local p value (Wilks 2016), thereby controlling the false discovery rates in multi-hypothesis testing with the Benjamini/Hochberg false discovery rate (FDR) algorithm. The corrected p values are then compared with the 5% global significance level.

4 Monsoon progression

4.1 Precipitation

Figure 2 shows the annual cycle of the monsoon (averaged between 8W and 6E) in terms of mean precipitation, wet-day intensity and wet-day frequency. A wet day is defined as a day with more than 1 mm of accumulated rainfall. The coast is located at approximately 5°N. CMORPH and TRMM show the oceanic and coastal phases of the monsoon from April to June, followed by the "monsoon jump" towards the end of June, when more intense rainfall starts in the Sahelian region with maximum rainfall around 12°N continuing towards the end of August. The monsoon gradually retreats

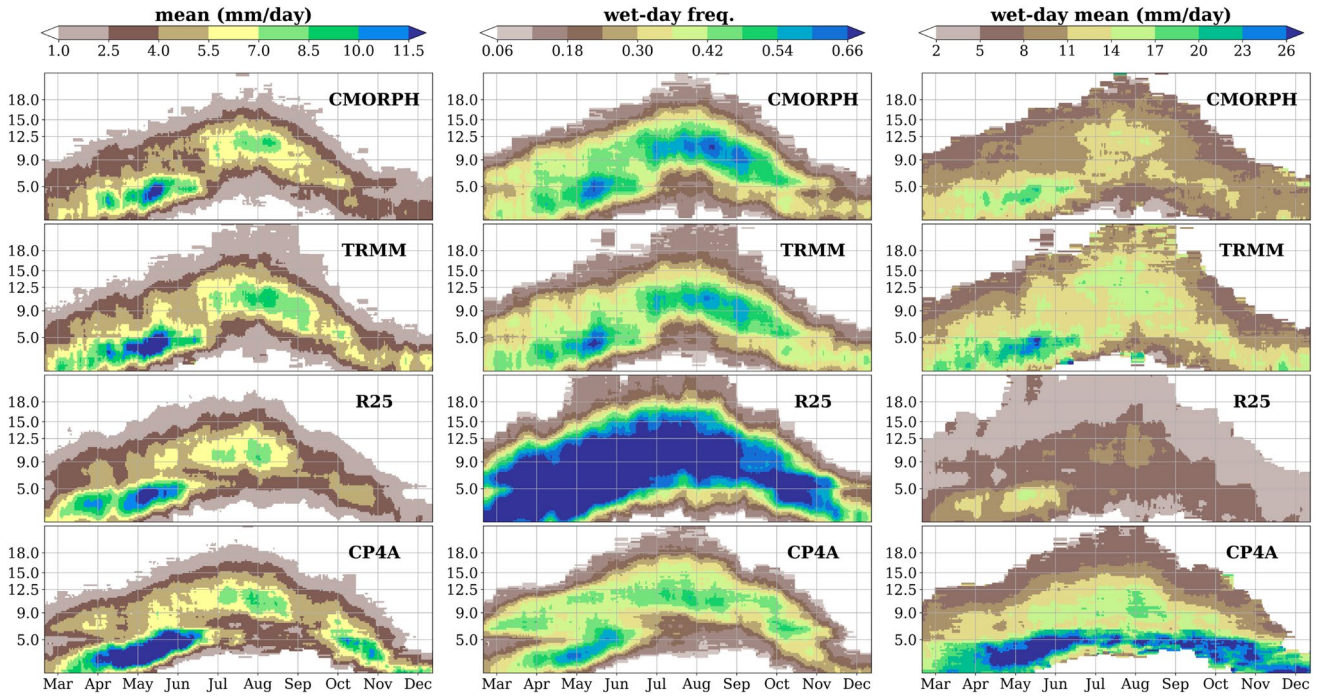

Fig. 2 Latitude-time evolution of (left) daily mean precipitation, (centre) wet-day frequency and (right) wet-day instensity averaged over 10 years and from 8W to 6E. A 10-day running mean has been applied

south from mid-September to the end of October. Precipitation frequency and intensity are maximum in April-June over the ocean and near the coast. Precipitation frequency is also large between 9 and 12.5°N in the Soudanian zone from July to September. During this period, precipitation intensity is largest around 12.5N with values reaching 11–14 mm/day in CMORPH and 14–17 mm/day in TRMM. Precipitation intensity is the main point of disagreement between the two datasets and it will be shown later that CMORPH is more reliable for this metric over land in this region.

The two models (R25 and CP4A) both show similar biases in the overall monsoon evolution (left hand panels). Rainfall starts too early in the Soudanian zone (June compared to July in the observations), making the monsoon jump a little less evident as rainfall occurs both over the ocean and over land during June and July. Another bias is an underestimation of rainfall in September and a slower monsoon retreat in October than in the observations. The largest differences between the two models are found in the precipitation intensity and frequency: R25 strongly overestimates the rainfall frequency and underestimates the rainfall intensity in all regions and seasons. Mean rainfall results from compensating biases in this model. In CP4A, rainfall frequency is much closer to the observations throughout the seasons and latitudes, although it tends to be 10–30% underestimated. Over land, CP4A is generally wetter than R25, which is a small ($\simeq$ 10–20%) improvement in July–September but a small deterioration in the shoulder seasons. Note that near 7–8°N, CP4A shows the well-know double peak in precipitation (May–June and October) both in terms of mean and frequency of precipitation as in the observations, whereas R25 has a weaker amplitude. In May and October, the overestimation of precipitation over land north of 9° in CP4A is mainly due to an overestimation of rainfall frequency. From June to September, CP4A has too strong precipitation intensity between 7 and 12.5° N.

Another notable difference between the models is the strong wet bias in CP4A over the ocean. It comes from a clear overestimation of rainfall intensity over the ocean and near the coast in May–June. When convection is triggered over the ocean, it is too strong. This is potentially a consequence of the lack of coupling between the ocean mixed layer and the atmosphere. Although R25 also has a prescribed SST, the convection scheme does not seem to be as sensitive to the lack of coupling as the explicit way of treating convection in CP4A. Another possible reason is that at 4.5 km the convection-permitting model does not correctly model shallow convection over the ocean and tends to have more precipitation from deep convection, in line with Becker et al. (2017) who found strong aggregation of convection when the convection scheme is switched off in radiative-convective equilibrium. Further

testing beyond the scope of our study is necessary to reduce this bias.

The monsoon retreat is also slower in both models; CP4A does not improve this. Zhang and Cook (2014) explain the delay in the demise of the WAM monsoon may partially be due to the North Atlantic subtropical high being too weak, which is the case in our global model (− 2 hPa in SON compared to ERA-interim, not shown).

4.2 Winds

The generally stronger mean rainfall from April to September in CP4A compared to R25, in the coastal region (5–9N) first and then in the Soudano-Sahelian region (9–15°N) is possibly explained by the stronger moisture convergence in convection-permitting models compared to convection-parameterised models in the Soudano-Sahelian zone (Marsham et al. 2013; Birch et al. 2014). Since the moisture convergence changes are mostly linked with low-level monsoon wind changes here we examine the 925 hPa meridional winds (Fig. 3a–c). In CP4A, the meridional winds are stronger between 5 and 9N from March to November and weaker between 9 and 18N from June to November compared to R25. These weaker winds start in June, when convection is triggered in the Soudanian zone. This clear pattern corresponds to the sketched explanation of Fig. 1 in Birch et al. (2014) and is explained below. Note that this makes the biases against ERA-interim larger in CP4A south of 9N but smaller between 9 and 15N from June to October (but note that ERA-interim 925 hPa wind fields will also be impacted by its convection-parameterisation, like R25 is, as explained below).

Figure 4 shows the diurnal cycle of the latitude distribution of mean precipitation and 925 hPa winds averaged between 8°W and 6°E and from July to September. Generally, night-time/morning precipitation is much better represented in CP4A than R25. Noticeably, the afternoon peak is shifted by about 3 h, although it is still too intense (see Sect. 7.2 for discussion about this). As illustrated by Fig. 4d–f, meridional moisture transport mainly occurs at night since dry boundary layer convection is strong during the day (Parker et al. 2005). From R25 to CP4A, the nocturnal jet in the Soudano-Sahelian zone (9–15N) in July–September is weaker and the the late afternoon/nocturnal jet in the Guinea coast zone (5–9N) is stronger. Birch et al. (2014) illustrated the following mechanism: since convection occurs later in the afternoon and during the night in convection-permitting models, there is more incoming

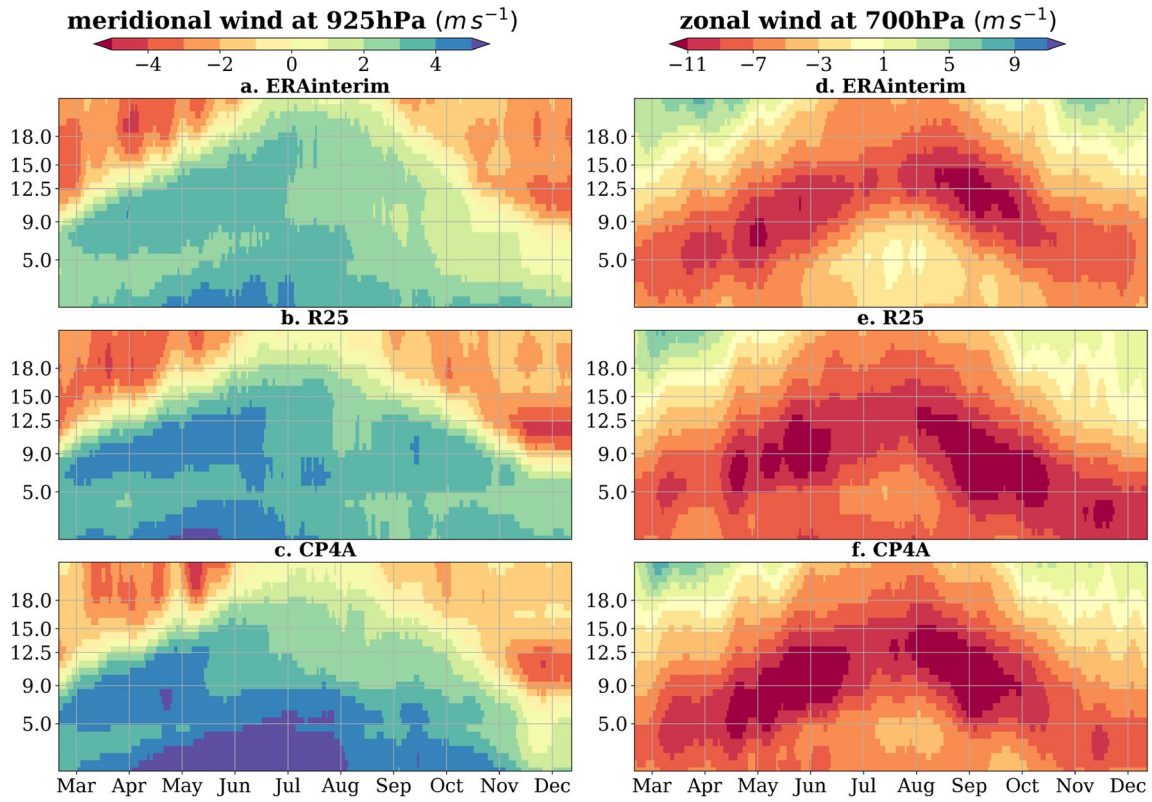

Fig. 3 Latitude-time evolution of (left) daily mean meridional wind at 925 hPa and (right) daily mean zonal wind at 700 hPa averaged over 10 years and from 8° W to 6° E. A 10-day running mean has been applied

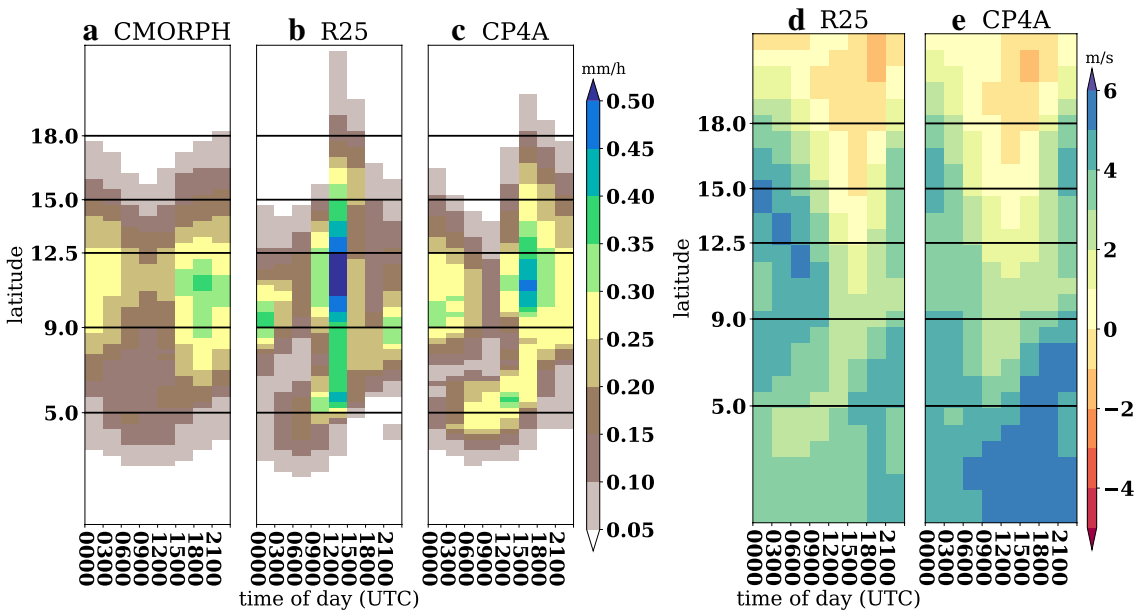

Fig. 4 Diurnal cycle of the latitude distribution of 3-hourly precipitation rate (mm/h) averaged between 8W and 6E in July–August–September for **a** CMORPH, **b** R25 and **c** CP4A and same diagnostic for the 3-hourly 925 hPa meridional wind (m/s) for **d** R25 and **e** CP4A

short-wave radiation during the day and convective warming at night. Consequently, they showed that night-time temperatures are warmer and surface pressure is weaker, reducing the pressure gradient relative to the Sahara and enhancing it relative to the coast. Furthermore, enhanced cooling in the Sahara by cold pool advection could also reduce the Sahel/Sahara gradient in the convection-permitting model (Marsham et al. 2013). This mechanism leads to stronger moisture convergence in the Soudano-Sahelian zone and allows CP4A to have stronger rainfall than R25. Birch et al. (2014) only investigated 40 days in the peak monsoon season. With the present study, we can confirm their findings and extend them: the fact that the northerly winds at 9–15°N start to be weaker from June, when convection occurs in the Sahel, adds to the evidence that convection is influencing low-level meridional transport. This effect is sustained during the whole monsoon season up to early November (Fig. 3).

Rainfall in April–May is also stronger in CP4A (Fig. 2). This is possibly linked with a stronger southerly flow in the coastal region compared with R25 (Fig. 3), although at that time of year, there is no corresponding reduction of southerly winds north of 9°N. Figure 5 indeed shows no change in the diurnal cycle of winds between R25 and CP4A north of 9°N, probably because convection is still weak in this region. However, winds are stronger in CP4A in the Guinea coast region from 18 to 03 UTC. A similar mechanism (warmer temperature at night increasing the pressure gradient at the coast) could be invoked. Future studies will need to investigate this in more detail.

June–September rainfall intensity north of the coastal zone (around 9°N) is also stronger than observed (Fig. 2, right panel). Another candidate to explain this is the African easterly jet (AEJ) shown in the 700 hPa zonal wind field (Fig. 3d–f). It is too broad and intense in both models compared to ERA-interim. Although the jet is slightly more constrained to the south in CP4A in JAS, it still appears too wide. Especially, it should be noted that the meridional shear on the southern side of the jet extends south to 5°N in the models but ends around 8°N in ERA-interim. Therefore, African easterly waves (AEW) could potentially occur further south in our models and together with stronger vertical wind shear between 5 and 9°N, could promote long-lived MCSs in this region in CP4A, which don't occur often in reality (Mohr and Thorncroft 2006; Maranan et al. 2018). Stronger convection in the early morning, which is an indicator of long-lived convective systems (Zhang et al. 2016a, b; Vizy and Cook 2018a), is indeed found both in July–August–September (Fig. 4) and April–May (Fig. 5) around 9–10°N.

To conclude this section, the most obvious added value from CP4A is the better representation of precipitation frequency and intensity and a shift to later precipitation during the day, which has consequences in terms of the diurnal cycle of the winds, which reinforces precipitation in CP4A. In the rest of the study, we investigate how CP4A represents precipitation in more detail at space- and time-scales potentially useful for users, to identify added value and remaining challenges for climate model developers. Although this added-value in terms of precipitation frequency and intensity is clear throughout the seasons over land, we focus on changes in the

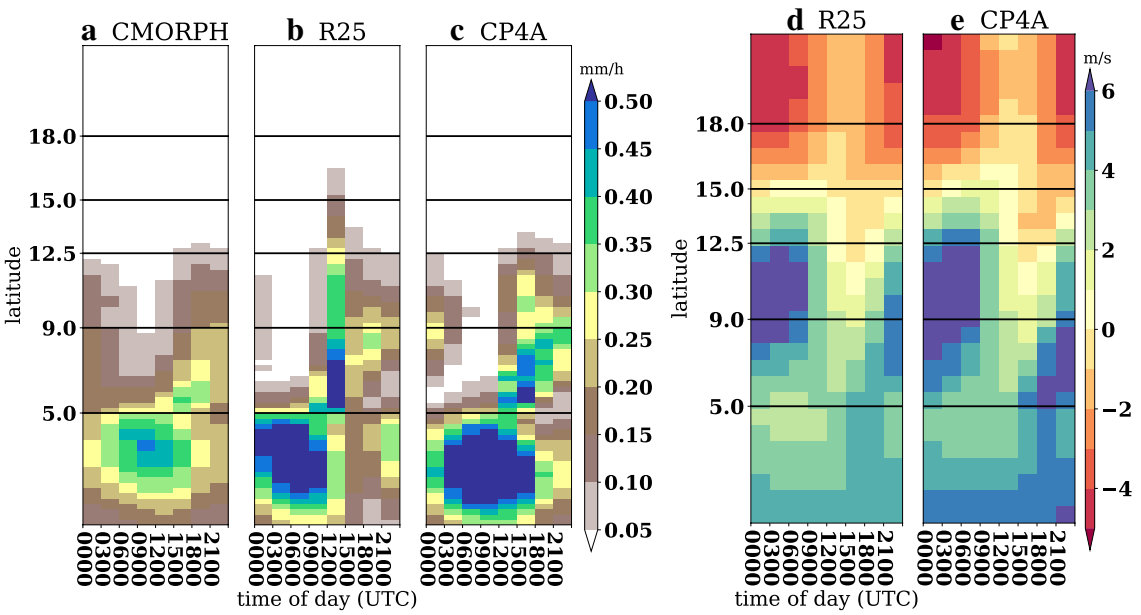

Fig. 5 Same as Fig. 4 for April–May

precipitation distribution in July–September for the sake of brevity and indicate when the changes differ in the shoulder seasons.

5 Spatial distribution of precipitation at the monsoon peak

Figure 6 further shows CP4A has a good representation of mean rainfall on flat land in the Soudano-Sahelian zone

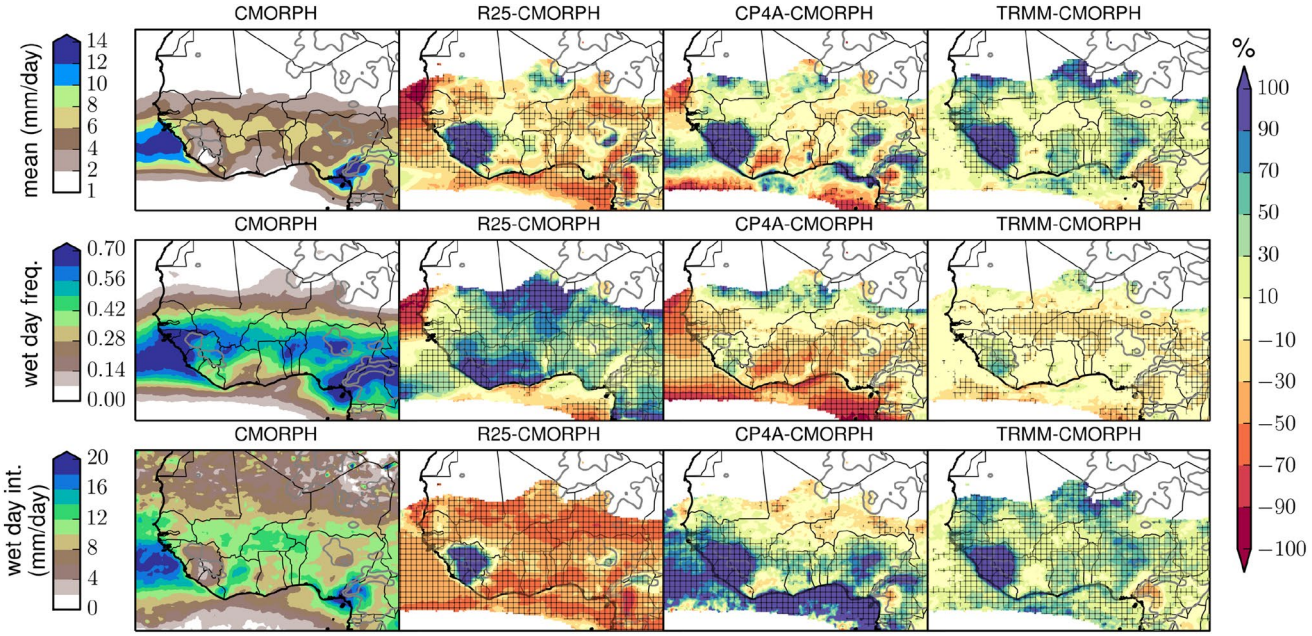

Fig. 6 Mean precipitation (mm/day, top), wet day frequency (centre), precipitation intensity on wet days (mm/day, bottom) in JAS for (left to right): CMORPH, R25-CMORPH, CP4A-CMORPH and TRMM-CMORPH in %. Areas where precipitation frequency is below 0.05 in CMORPH are masked out in white in the difference plots. Stippling shows the significant values at the 5% global level, as explained in Sect. 3.3

between 8W and 6E, compared to R25 which has a 10–30% dry bias. This finding can be extended to most low-land areas except over the Ivory Coast. Note that in Guinea, Sierra Leone and Liberia, CMORPH shows a strong underestimation compared to other datasets (Sect. 3.2), so we will not discuss model performance in these regions. It is again striking that CP4A has a better representation of the wet-day frequency and wet-day intensity than R25 in all regions. R25 has 30–90% too many wet days and a precipitation intensity 30–70% too low. CP4A has a much smaller but opposite bias of too intense and infrequent rainfall in the Soudanian and Guinea coast zone, potentially linked with a too broad AEJ as explained earlier. There is also a remaining dry bias along the Guinea coast, where the "little dry season" is too dry by 30–70% (especially in Ivory Coast). We speculate that this could be linked with an incorrect orientation of the flow at the coast near Cape Palmas or too strong southerlies exporting moisture north as shown in Fig. 3. This also needs further investigation in following studies.

CP4A shows a clear overestimation of precipitation intensity on wet-days over the orography (Jos Plateau, Cameroun Line Mountains). Figure 7 compares mean precipitation using different datasets. Although these datasets are not independent (e.g. TRMM is corrected against GPCC and CMORPH against CPC which has a similar station network as used in ARC2, CHIRPS includes TRMM and a previous version of CMORPH in its climatology), none of them shows as much precipitation over the orography as CP4A. CHIRPS, which includes fine-scale terrain-induced precipitation enhancement in its baseline climatology (Funk et al. 2015b), shows the highest rain rates over the orography. However, although we can't rule out a systematic underestimation of orographic precipitation because of scarce station data at higher elevation, it is likely that CP4A overestimates orographic precipitation. A similar bias (although smaller) was found in Europe over the Alps against much higher-density datasets by Berthou et al. (2018). Note that over lower mountains such as the 500–900 m Togo-Atakora mountains, mean precipitation is in good agreement with CMORPH, ARC2 and CHIRPS.

Note that these points are also valid for April–June and October–November. The main difference is that the band of too intense precipitation in CP4A around 9°N is shifted south by about 1° and the overestimation of precipitation north of this band is due to too large rainfall frequency.

6 Daily and sub-daily precipitation distributions

6.1 On a 25 km grid

6.1.1 Model evaluation

Distributions of 3 hourly precipitation on a 0.25° grid are presented in Fig. 8. They are plotted in terms of contribution to mean precipitation with near-exponential bins as detailed in Klingaman et al. (2017) and further explained in Berthou et al. (2018) and in the caption of Fig. 8. The distributions are presented for different regions to account for the strong spatial variability across West Africa (see Fig. 1):

1. SEN, mostly covering Senegal, which is under the influence of east–west traveling MCSs and of the Atlantic ocean,
2. NSA, northern part of the Sahelian zone at the edges of the Sahara with weak mean precipitation.

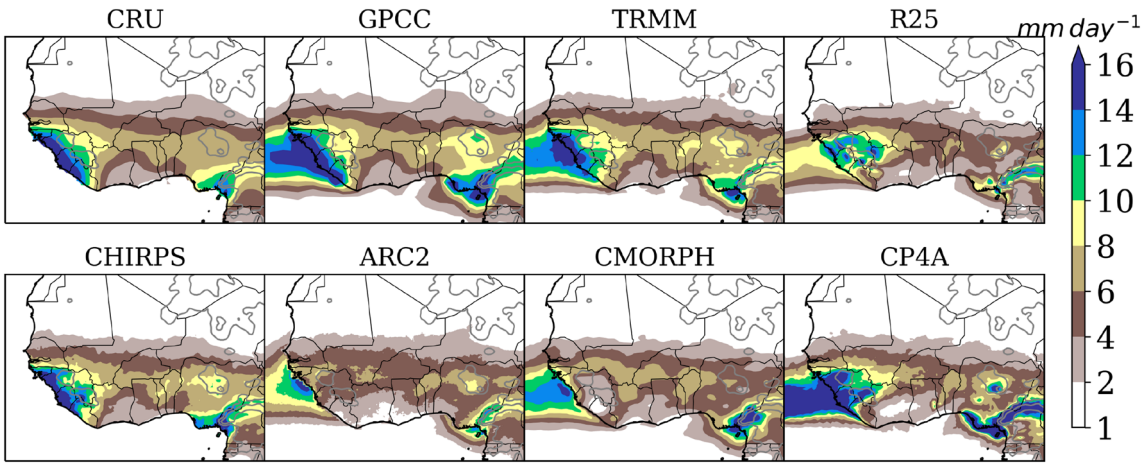

Fig. 7 Mean precipitation (mm/day) in JAS for different datasets

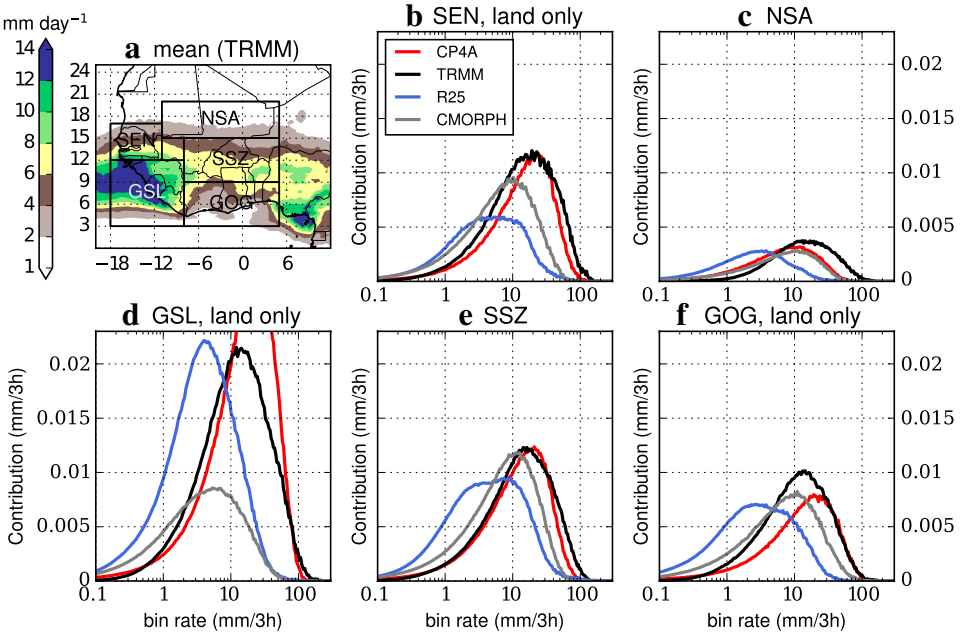

Fig. 8 3-hourly precipitation contributions to mean precipitation rate in JAS over the regions named in the top-left corner for TRMM, CMORPH, CP4A and R25 regridded on a 0.25° grid. Precipitation rates are binned with near-exponential bin sizes [see Klingaman et al. (2017) for the exact formula] to account for more frequent rain events at low rain rates. Then, each bin frequency is multiplied by the mean bin rate: summing across the bins will give the mean precipitation rate of the region. The x axis is plotted on a log scale and the y axis on a linear scale to compare the bulk of the distribution

3. GSL, mostly covering Guinea, Sierra Leone and Liberia, under the influence of the monsoon flow and strong orographic forcing,
4. SSZ, covering the Soudanian zone and southern part of the Sahelian zone, away from direct orographic influence,
5. GOG, covering southern coastal areas encountering a little dry season in JAS,

In all regions, CP4A and R25 have very different precipitation distributions: R25 shows a larger contribution from events below 5–8 mm/3 h compared with CP4A and little contribution to mean precipitation from rates larger than 20 mm/3 h. This is coherent with Pearson et al. (2014), who showed that 95% of precipitation in a previous version of the UM convection-parameterised model came from the convection scheme. CP4A is always in better agreement with TRMM and this is also true compared with CMORPH except in GSL and SEN regions. The best agreement of CP4A with CMORPH is in northern Sahel. In SSZ, CP4A is in good agreement with TRMM but compared with CMORPH overestimates precipitation rates above 15 mm/3 h and underestimates precipitation below this threshold. In GOG, CP4A underestimates precipitation below 15–30 mm/3 h compared to CMORPH and TRMM, which leads to the dry mean bias at daily time scales. The higher end of the distribution is aligned with TRMM but the contribution of rates larger than 15 mm/3 h is too large compared to CMORPH. Note that this bias is also seen at the daily scale in Fig. 6 with too few wet-days and a too large wet-day intensity. Since CMORPH is in better agreement with local observations in SSZ (see Sect. 6.1.2), it is likely that CP4A overestimates intense precipitation and underestimates weaker precipitation in SSZ and more strongly so in GOG. As explained in Sect. 4, this may be linked with the extension of the AEJ too far south in the models, which potentially favours strong convection around 7°N–12°N. Some of the contribution may also come from strong convection over Lake Volta in eastern Ghana as shown in Fig. 7. Overall, CP4A is showing a much better precipitation distribution than R25, with stronger precipitation events contributing to mean precipitation.

Figure 9 similarly shows that the more intense values of daily precipitation are better represented in CP4A, although they are too intense against CMORPH by 10–70% in the Soudanian zone. If TRMM is taken as a reference around the Guinea mountains, there is also an improvement in CP4A, although intense precipitation is overestimated by 30–50%. The underestimation of this metric against TRMM in the northern part of the Sahel seems to be less reliable, since TRMM overestimates strong precipitation in this region (see next section). The overestimated intensity of strong rainfall events in the Soudanian zone could be linked to a too strong AEJ south of 12°N (Sect. 4), which could promote long-lived types of MCSs, mostly absent from this region in observations (Maranan et al. 2018).

Finally, Fig. 10 shows the joint probability distribution of wet spell duration and mean rainfall intensity in the NSA, SSZ and GOG regions. A wet-spell is defined as consecutive 3 h intervals with rainfall rate above 0.1 mm/h. This figure further illustrates that R25 shows too many low-intensity

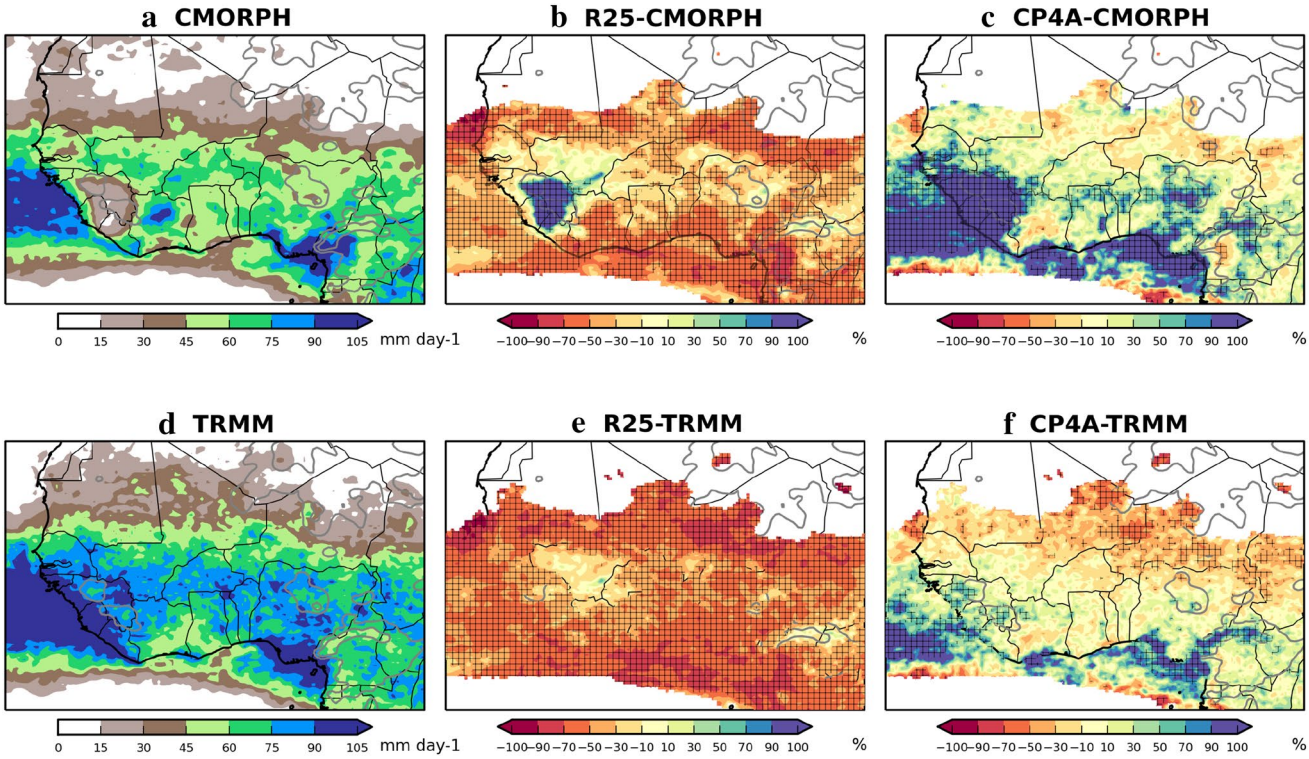

Fig. 9 Average of values over the 99th centile of daily precipitation in JAS on a 0.25° grid for **a** CMORPH, **b** R25-CMORPH, **c** CP4A-CMORPH, **d** TRMM, **e** R25-TRMM, **f** CP4A-TRMM. This corresponds to the average intensity of the top 9 daily events in each grid point. Stippling shows the significant values at the 5% global level as explained in Sect. 3.3

rainfall wet-spells (< 6 mm of cumulated rain) in all duration bins and not enough intense wet-spells from 6 to 150 mm. CP4A shows a shift to overall fewer wet-spells, which are more intense and short-lasting. As also noted in Fig. 8, CP4A agrees better with TRMM in the GOG and SSZ regions and with CMORPH in the NSA region. Generally, the large rainfall amounts happen in shorter wet-spells in CP4A compared to CMORPH (e.g. very few events with amount larger than 15 mm and duration longer than 9 h in CP4A in SSZ and GOG). Moreover, intense wet-spells (> 30 mm/h) can have longer durations in GOG than in SSZ, in line with Maranan et al. (2018) who showed that organised convective systems propagate at a slower speed in the SSZ region. CP4A does show this behaviour but to a lesser extent than observations. It also shows too many long-lasting very intense wet-spells (> 60 mm, > 3 h), especially in GOG. Crook et al. (2019) also found that the contribution to mean precipitation by long-lasting (> 9 h, in a lagrangian definition) and slow (< 8 m/s) MCSs was too large in this region in CP4A, which could be related to this. The lack of weaker events (< 15 mm) in GOG in CP4A is especially large for events lasting more than 3 h. CP4A also overestimates the short (0–3 h) wet-spells in all regions compared to CMORPH, which is potentially partly linked with its too strong diurnal cycle (see Sect. 7).

Overall, CP4A has a very good distribution in Northern Sahel but overestimates intense and short-lasting wet-spells and underestimates low-intensity events of all durations against CMORPH in SSZ and GOG. The dry spells, using a simple 1 mm/day threshold, are also generally longer and more numerous in CP4A compared with R25, closer to the observations except in the GOG region, where CP4A shows too many long-lasting (> 5 days) dry spells (not shown). Similarly, CP4A shows better performance than R25 for RX1 (10-year median of the maximum seasonal precipitation in 1 day), RX5 (10-year median of the maximum seasonal precipitation in 5 days), CDD (10-year median of the maximum number of consecutive dry days in one season) and CWD (10-year median of the maximum number of consecutive dry days in one season) (not shown). CP4A remaining biases in the south of the region and over the orography (too strong intensity and too small frequency of rainfall) are affecting these variables (not shown).

6.1.2 Satellite dataset quality

Dataset quality was already discussed regarding the SEN and GSL regions in Sect. 3.2. To further check satellite dataset quality in other regions, Fig. 11a, c and e show the comparison of CP4A, TRMM, CMORPH and the rain-gauge based

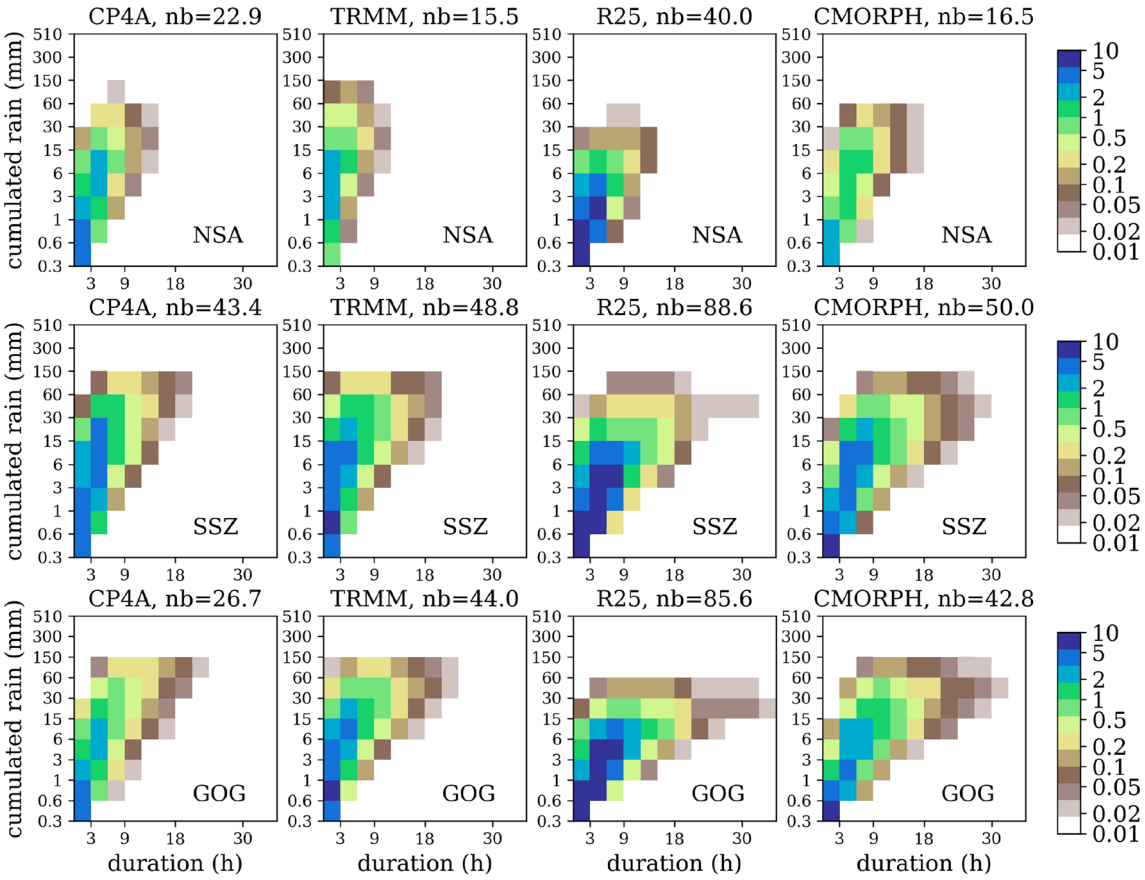

Fig. 10 Number of wet-spells per season (in JAS) and per 0.25° grid-point in different duration and cumulated rainfall categories. Top is for the NSA region, middle for the SSZ region and bottom the GOG region (defined in Fig. 8) for the four datasets as indicated in the titles. The number written above the plots is the average number of wet spells per grid point per season. Note the colorbar is log scale

dataset AMMA-CATCH on the three mesosites (location presented in Fig. 1). All datasets are 3-hourly and regridded on TRMM grid (0.25°) in these panels. CMORPH shows very good agreement with AMMA-CATCH on the three sites. CP4A also shows very good agreement with AMMA-CATCH-Mali and AMMA-CATCH-Niger (the first one is in NSA and the second one in the north of SSZ), but in Benin has much fewer low-intensity precipitation and too much high intensity precipitation compared to AMMA-CATCH-Benin, similarly to TRMM, as shown in the averaged SSZ and GOG regions of Fig. 8. CMORPH seems more reliable than TRMM in the NSA and SSZ regions and was therefore chosen as a reference dataset in Figs. 2 and 6, although it shows other drawbacks over the Guinea mountains as discussed earlier and in Sect. 3.2.

6.2 On a 4 km grid

Although a model is not supposed to represent well the atmospheric processes at its grid scale (Skamarock 2004), some users such as hydrologists may ideally like to use the fine temporal and spatial scales provided by CP4A and it is further important to evaluate it from a model development perspective. The AMMA-CATCH dataset provides a good evaluation tool in this regard: the 15 mn- and 3 hourly precipitation can be evaluated on a 4 km grid in Fig. 11b, d and f. Comparing the left panels and the right panels for AMMA-CATCH-3h and CP4A-3h, the only difference is the spatial scale: on the left, precipitation is on a 25 km grid and on the right it is on a 4 km grid. This shows that CP4A is in good agreement at 3-hourly time-scale and 25 km scale with AMMA-CATCH-Mali and Niger, but precipitation comes from too intense events on a 4.5 km grid at 3-hourly time-scale. In all three sites, CP4A peak is shifted to higher values on the 4.5 km grid and lighter precipitation is underestimated compared to AMMA-CATCH. This suggests that precipitation systems are too intense and localised on a 4.5 km grid but aggregate well at 25 km scales. This is a known problem of the model when analysed on its native grid and it was evaluated that resolutions of about 200 m would be required to solve this problem (Hanley et al. 2015; Stein et al. 2015a).

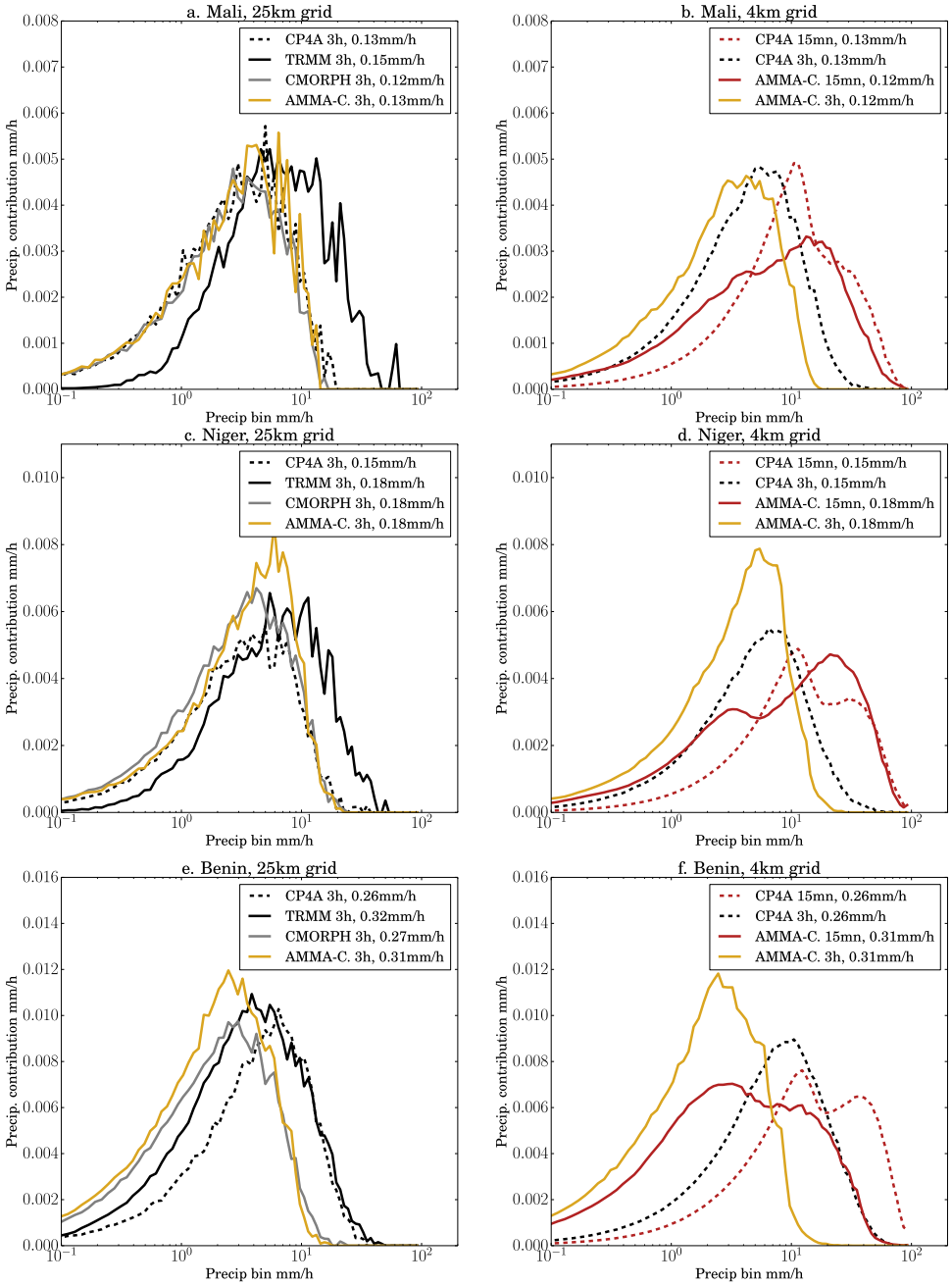

Fig. 11 3-hourly precipitation contributions to mean precipitation rate (mm/h) in JAS on a 0.25° grid (left) and 3-hourly/15-mn precipitation contributions to mean precipitation rate on a 4 km grid (right) for the three AMMA-CATCH mesosites: **a**, **b** Gourma (Mali), **c**, **d** Niamey (Niger), **e**, **f** Ouémé (Benin). Mean precipitation rate (sum across all bins) is indicated in the legend box. **a**, **c**, **e** Are similar to Fig. 8 but for the mesosites instead of the wider regions. The mesosite locations are indicated in Fig. 1

At a 15 mn scale, a similar bias is also present in Benin and Mali, but in Niger the differences are tripolar (underestimation of precipitation below 6 mm/h, overestimation between 6 and 15 mm/h and underestimation between 15 and 50 mm/h). The precipitation contribution represented this way has two peaks: the peak at stronger values dominates in AMMA-CATCH while the peak at weaker values is dominant in CP4A. This may be related to the convective and stratiform parts of precipitating systems, which may have different shares in CP4A compared to AMMA-CATCH. Table 1 gives further information on the spatial characteristics of rainfall in CP4A compared to the rain-gauge network of the Niamey mesosite in Niger, for 1997–2006 from July to September. Large-scale precipitation systems are defined as covering at least 30% of the 30 rain-gauges in AMMA-CATCH and of the 625 grid points in CP4A. Their number is in very good agreement between CP4A and AMMA-CATCH. On this mesosite, 96% of precipitation comes from these large-scale systems in AMMA-CATCH. This fraction is 86% in CP4A, due to both the underestimation of large-scale event mean intensity (by 30%) and the overestimation of the number of small-scale events (by 59%) and their intensity (by 56%). The mean inter-event time and the mean size of the

Table 1 Mean number of events per year and mean annual rainfall by event type at Niamey mesosite (Niger) in JAS (1997–2006)

	Mean annual number of events			Mean annual rainfall (mm)		
	Total	Large events	Small events	Total	Large events	Small events
AMMA-CATCH	49	32	17	402	385	17
% of total	100	65	35	100	96	4
CP4A	57	30	27	311	269	42
% of total	100	53	47	100	86	14

For AMMA-CATCH, a minimum threshold of 1 mm at at least two stations define an event. For CP4, there is no minimum threshold. Events are separated by a minimum of 30 min. Large events are given when at least 30% of stations/grid-points recorded more than 0.5 mm of rainfall

Table 2 Inter-event time: days between each event, measured from beginning of one event to the beginning of the next

	Inter-event time (days)	Event size (ratio)	Event intensity (mm)
AMMA-CATCH mean	1.88	0.58	11.1
AMMA-CATCH std	1.57	0.34	9.1
CP4A mean	1.62	0.67	6.8
CP4A std	1.25	0.25	6.5

Event size: values are in proportion of stations/data points measuring precipitation. Event intensity: average rainfall per station per event. All values are for July–August, averaged over 1997–2006 for the Niamey mesosite (Niger). Note that AMMA-CATCH has 30 stations whereas CP4 has 625 points over the same area

precipitation systems is in good agreement (only different by about 15%) between CP4A and AMMA-CATCH (Table 2), although the mean intensity is underestimated by about 38%, which is in the same range as Fig. 6 at the daily time-scale against CMORPH. Figure 11d shows that this underestimation mainly comes from precipitation rates between 15 and 50 mm/h being underestimated, although 6–15 mm/h precipitation is overestimated.

7 Diurnal cycle and MCSs

7.1 Better diurnal cycle in CP4A

Zhang et al. (2016a) showed that the diurnal cycle in TRMM had a single peak at most grid-points and has a strong spatial variability. Therefore, to avoid averaging over given regions, we use a harmonic fit of the 3-hourly datasets and diagnose the hour of maximum precipitation and the amplitude of the harmonic (Fig. 12). Three quantities can be compared between the models and the observations: the area where the harmonic fit is not good ($R^2 < 0.5$), shown in grey, the amplitude of the harmonic (a–d) and its phase (e–h). First, CP4A has larger areas where the harmonic fit is suitable for the diurnal cycle (less grey area) than R25, quite similar to the observations. Figure 4 indeed shows that R25 has a very strong peak around midday, and a cosine fit is likely a sub-optimal estimation of this behaviour.

Second, the largest amplitude of the diurnal cycle is found over the orography (except in CMORPH over the Guinea mountains) and offshore the western coasts of GLS and Nigeria/Cameroon. Precipitation is maximum in late afternoon over the orography. This is well reproduced in both R25 and CP4A models, although R25 tends to have an earlier precipitation peak and CP4A a stronger amplitude.

Third, over flat land in the Sahel region, CP4A is superior to R25 in both phase and amplitude of the diurnal cycle. Its amplitude is quite similar to TRMM but still overestimated compared with CMORPH. The timing of maximum precipitation is too early in R25, which is a well-known behaviour of the convective parameterisation (e.g. Martin et al. (2017); Trenberth et al. (2017)). CP4A still peaks too early, but note that CMORPH and TRMM tend to have too late a peak compared to AMMA-CATCH observations by about 2 h (Pfeifroth et al. 2016). Indeed, CP4A agrees better with AMMA-CATCH than TRMM and CMORPH in Benin where the afternoon peak is dominant (not shown). However, CP4A has a more spatially homogeneous timing of precipitation than both datasets in the Sahel: it occurs mainly between 4 pm and 8 pm. The early morning peak over Niamey (Niger, blue/green colours), shown in the observations (and in AMMA-CATCH, not shown) and the east–west gradient from the Jos Plateau to Niamey are not well represented in CP4A. Note that these are due to travelling MCSs generated both over the Jos Plateau/AÏr mountain orography and the Damergou gap Vizy and Cook (2018a). The daytime peaks in Burkina Faso and eastern Niger/Nigeria were explained by Vizy and Cook (2018b) by local triggering of convection in different circumstances in both regions and by the travelling long-lived MCSs also triggered in the Damergou gap.

Nevertheless, patterns in coastal countries are well captured by CP4A: the night-time peak of precipitation over Eastern Senegal and Ivory Coast, and the early morning peak between the Jos Plateau and the Cameroon Line mountains.

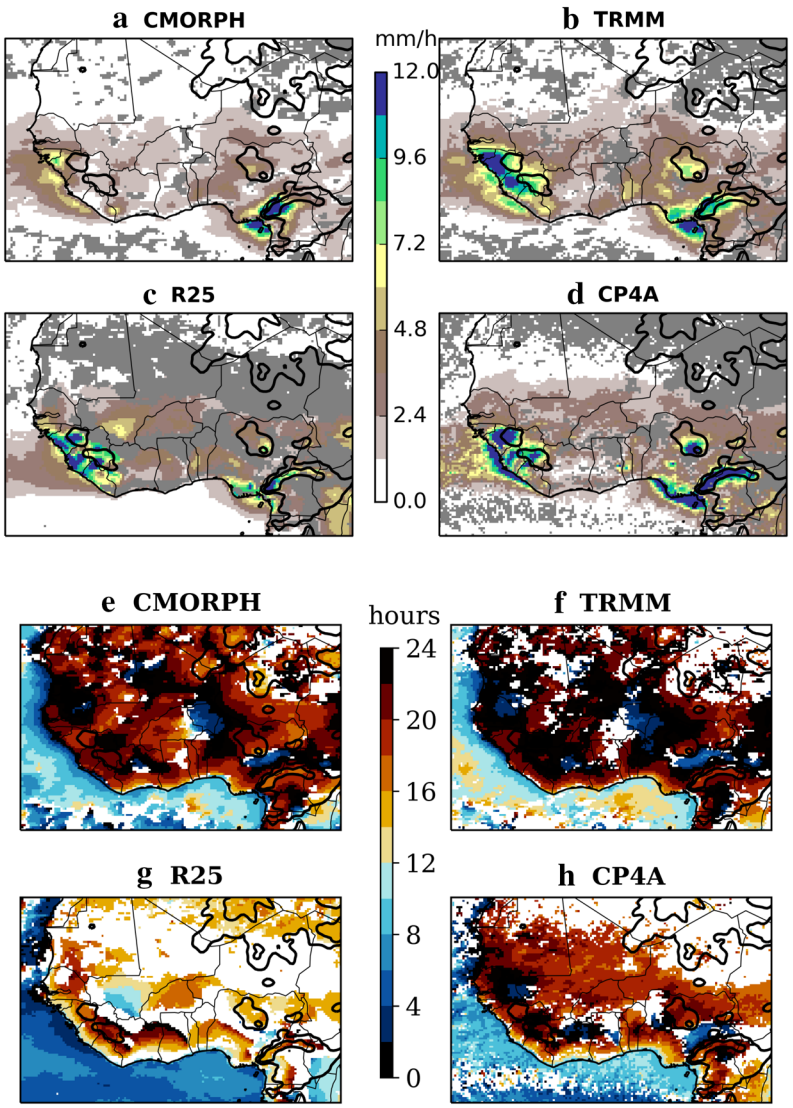

Fig. 12 **a**–**d** Amplitude of the harmonic fit to the diurnal cycle of precipitation in JAS (mm/h); **e**–**h** phase (hour of maximum) of the harmonic fit to the diurnal cycle (local time) in JAS. Areas where the goodness of fit $R^2 < 0.5$ are masked in grey in panels **a**–**d** and in white in panels **e**–**h**

On the southern coast, there is a gradient in peak rainfall from 06 to 09 UTC at the coast to later afternoon peak around 6°N, as also indicated by Fig. 4a–c. This pattern, present both in the observations and the models, clearly shows the signature of sea breeze. This is not so clear from the wind intensity (Fig. 4d–f) but Parker et al. (2017) explain that the sea breeze does not behave as a gravity current since the monsoon flow is strong but rather as a deepening of the boundary layer from the coast to inland. As shown in Fig. 4a–c, the morning peak in precipitation in CP4A is overestimated over the sea and coast. The inland penetration is also too large: up to 7°N in both R25 and CP4A against 6°N in CMORPH and Fig. 4.18 of Parker et al. (2017).

From Fig. 5, most of these conclusions are also valid in April–May: the precipitation signature of the sea breeze in even stronger than in JAS in both the observations and the models.

Note also the early morning peak of precipitation over Lake Volta in CP4A, which is not present in CMORPH and TRMM but also reported by Parker et al. (2017) in terms of cloudiness (in their Fig. 4.18).

Overall, CP4A is better able to reproduce the shape, timing and amplitude of the diurnal cycle than R25 away from the orography. It is able to reproduce the spatial structure of the phase around the orography and in coastal countries but not in the Sahel.

7.2 Still too much non organised convection

In this section, we seek to understand the diurnal cycle biases in CP4A.

Stratton et al. (2018) showed by means of a Hovmöller diagram on 1 month (Fig. 9 of their article) that westward propagating MCSs are well represented in CP4A but smaller-scale slow moving diurnal precipitation is too intense. To

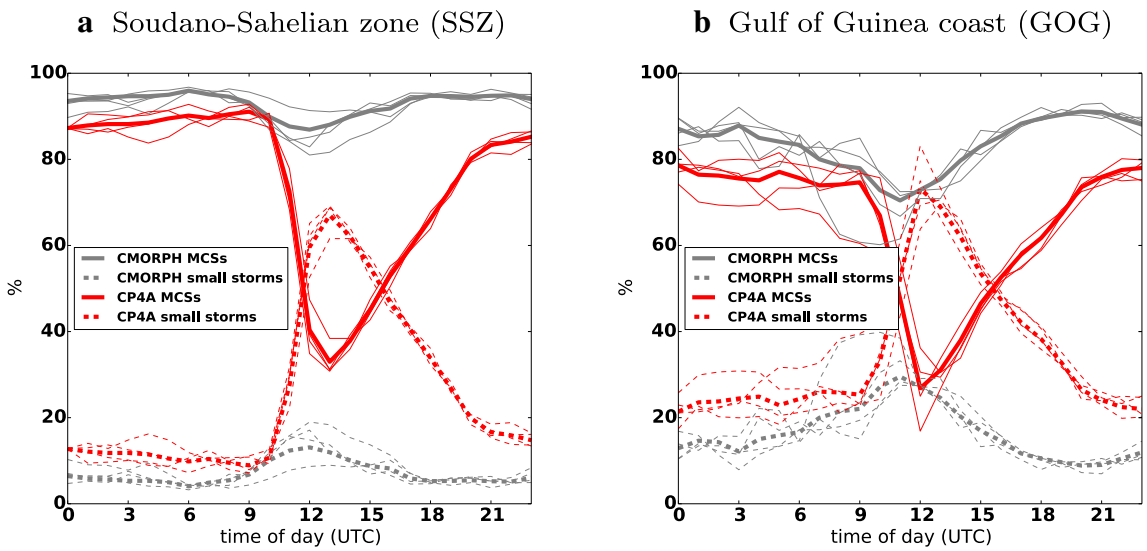

Fig. 13 Contribution to mean hourly precipitation rate (%) by time of day for small storm clusters (< 1000 km^2) and MCSs (> 1000 km^2); **a** for the SSZ region and **b** for the GOG region. Thick lines are the 4-year averages and thin lines represent individual years

quantify this behaviour, Fig. 13a shows the contribution of precipitation to mean diurnal cycle by storm type: small storms and MCSs are differentiated by a size threshold of 1000 km^2. This is determined using the tracking of precipitation objects described in Sect. 3.3. This figure shows that night-time/morning precipitation mainly results from MCSs (over 90% in CMORPH) and that small storm contribution is maximum around midday, representing 15% of rainfall at that time in CMORPH. In CP4A, this midday peak of small-scale storm contribution occurs later and is much stronger than in CMORPH: up to 65% of the rainfall at 2 pm comes from small storms. Therefore, the too early peak of total precipitation in CP4A in the Sahel and probably the more homogeneous spatial structure of the hour of maximum precipitation is related to too large a share of diurnal small-scale convection compared to MCSs in the precipitation mean rate. Although different years were used in CP4A and CMORPH to do the tracking, this particular model bias is much larger than year-to-year variability, as shown by individual years (thin lines in Fig. 13). This is also consistent with the comparison against AMMA-CATCH, using different criteria (Sect. 6.2 and Table 1): it also showed too much small-scale convection but the right number of large-scale events. The good number of MCSs is consistent with the presence of a night-time peak of correct intensity in CP4A in Fig. 4. Note that this is an opposite bias to Zhang et al. (2016b), who found that diurnal convection is not triggered enough in their CPM, and they link it with too high a boundary layer. In CP4A, this behaviour may be related to the use of stochastic perturbations in the boundary layer scheme, which may require some tuning down for this region.

Moving south to the GOG region (Fig. 13b), the share of small-scale convection is larger in GOG than in SSZ, as also shown by Maranan et al. (2018): it grows from 15% at midnight to 25% around midday. CP4A also has a similar share in the morning (20%) but again the afternoon peak is overestimated (up to 75% of total rainfall at this time of day).

8 Conclusion

We present a comparison of a 10-year 4.5 km convection-permitting model (CP4A) with a 25 km × 40 km regional simulation using a convective parameterisation (R25) in terms of their representation of the West African monsoon. Both simulations were driven by a present-day atmosphere-only GCM at 25 km × 40 km and cover a pan-African domain. Overall, CP4A shows substantial improvements compared to R25 in terms of precipitation:

- improved wet-day frequency and intensity,
- improved distribution of 3-hourly precipitation, with very good agreement in the Sahelian zone (12.5–18N)

against CMORPH and AMMA-CATCH on a 25 km grid,
- better representation of dry and wet spells
- better representation of the diurnal cycle and of its spatial variability around the coasts and orography.
- good representation of the size and number of large-scale MCSs compared with AMMA-CATCH Niamey in JAS. Crook et al. (2019) will provide more in-depth analysis of MCSs.
- reduced mean bias over the Sahelian region in JAS, from 10 to 30% to typically less than 10%.

Nevertheless, CP4A still shows the need for further model improvements:

- the monsoon progression is relatively similar to R25 and the driving model, starting too early and ending too late, the wet biases in April–May and October are stronger in CP4A, potentially linked with too strong late evening monsoon flow from the ocean to the coast in these seasons.
- from 7°N to 12.5N (Soudanian zone and just south of it), heavy rainfall is too intense and frequent and low-intensity rainfall is not frequent enough, with an overall dry bias in these regions. This could be at least partly related to the too broad AEJ in both models, with the meridional gradient of the zonal wind reaching the coast in the models.
- in the Sahelian zone away from the orography, small-scale diurnal convection contributes too much to total precipitation and this leads to a diurnal phase which is too homogeneous in this region. This could be tested in short simulations and potentially be corrected by reducing the amplitude of stochastic perturbations in the boundary layer.
- precipitation is too intense over the orography and over the ocean. We speculate that the latter could be reduced by the coupling with an ocean slab model.
- if analysed on a 4.5 km grid, precipitation is too intense (low-intensity precipitation rates are underestimated, high intensities most often overestimated, except in Niger at 15 mn time-scale.). This suggests that CP4A output should not be used on its native grid to drive hydrology or crop-models, or should first be bias-corrected.

Although we used the closest model set-up as possible, R25 and CP4A still have a few other differences than just changing resolution and switching off the convection scheme. They have some influence on our results that we could not quantify in this study.

Nevertheless, results from shorter month-long simulations such as the Cascade project are confirmed and extended to other seasons using a 10-year mean: the better diurnal cycle of convection in CP4A influences the diurnal cycle of wind, with stronger moisture convergence in the Sahel from June, when convection starts in the Soudano-Sahelian zone. This leads to stronger moisture convergence in the Sahel and increased precipitation in CP4A. In April–May, the monsoon flow at the coast is also enhanced at night in CP4A, probably leading to a worsening of the wet bias in this season. Future studies such as the Coupling of convective rainfall and temperature gradients in a warming climate (CLOVER) within the AMMA-2050 project will investigate in more details the representation of monsoon processes in the Gulf of Guinea coastal region.

Unlike mid-latitude regions, where CPMs add value for the precipitation field mainly on the sub-daily time-scale (Liu et al. 2016; Berthou et al. 2018), this CPM shows much larger improvements in the distribution at both daily and sub-daily scales when analysed at 25 km scale. However, it should be noted that improvements in the parameterisations are on-going to take into account the problems highlighted in this study. Furthermore, research is on-going to include a scale-aware convection parameterisation, which would potentially be able to produce more light-precipitation in convection-permitting models.

This article highlights that CP4A is more suitable than R25 in representing precipitation at both time and space scales which are very important from a user-perspective, due to the better representation of MCSs. We can therefore expect CP4A to give more reliable user-relevant climate change information about intense rainfall, wet/dry spells and evolution of MCSs in this region. Future study will analyse how different the climate change signal is between R25 and CP4A.

Acknowledgements The research leading to these results received funding from the UK National Environment Research Council (NERC)/ Department for International Development (DFID) FCFA programme, under the AMMA-2050 project (Grant numbers NE/M019977/1 and NE/M019969/1) and the Joint UK BEIS/DEFRA Met Office Hadley Centre Climate Programme (4A01101). J. Crook received funding from the NERC Vegetation Effects on Rainfall in West Africa (VERA) project (Grant number NE/M003574/1). The AMMA-CATCH regional observing system was set up thanks to an incentive funding of the French Ministry of Research that allowed pooling together various pre-existing small scale observing setups. The continuity and longevity of the measurements are made possible by an undisrupted IRD funding since 1990 and by a continuous CNRS-INSU funding since 2005. Output from the model simulations will be made publically available in July 2019 (Stratton et al. 2018). The authors are thankful to R. Schiemann who provided the initial version of the code for the diurnal cycle analysis and to G. Martin who provided the ASoP-spectral code available at https://github.com/nick-klingaman/ASoP/tree/master/ASoP-Spectral. All figures were produced using Matplotlib 1.3.1 and Iris 2.0 Met Office. git@github.com:SciTools/iris.git.

References

AMMA-CATCH (1990) AMMA-CATCH observatory: Niamey square degree mesoscale site (16,000 km^2) in the cultivated Sahelian zone, Niger. Tech. rep., IRD, CNRS-INSU, OSUG, OMP, OREME. https://doi.org/10.17178/AMMA-CATCH.niger

AMMA-CATCH (1996) AMMA-CATCH observatory: upper Oueme mesoscale site (14,000 km^2) in the sudanian climate zone, Benin. Tech. rep., IRD, CNRS-INSU, OSUG, OMP, OREME. https://doi.org/10.17178/AMMA-CATCH.benin

AMMA-CATCH (2003) AMMA-CATCH observatory: Gourma mesoscale site (30,000 km^2) in the Sahelian pastoral zone, Mali. Tech. rep., IRD, CNRS-INSU, OSUG, OMP, OREME. https://doi.org/10.17178/AMMA-CATCH.mali

Aranami K, Davies T, Wood N (2015) A mass restoration scheme for limited-area models with semi-Lagrangian advection. Q J R Meteorol Soc 141(690):1795–1803. https://doi.org/10.1002/qj.2482

Becker T, Stevens B, Hohenegger C (2017) Imprint of the convective parameterization and sea-surface temperature on large-scale convective self-aggregation. J Adv Model Earth Syst 9(2):1488–1505. https://doi.org/10.1002/2016MS000865

Berthou S, Kendon EJ, Chan SC, Ban N, Leutwyler D, Schaer C, Fosser G (2018) Pan-European climate at convection-permitting scale: a model intercomparison study. Clim Dyn. https://doi.org/10.1007/s00382-018-4114-6

Birch C, Parker D, Marsham J, Copsey D, Garcia-Carreras L (2014) A seamless assessment of the role of convection in the water cycle of the West African monsoon. J Geophys Res 119:2890–2912. https://doi.org/10.1002/2013JD020887

Boutle IA, Eyre JEJ, Lock AP (2014) Seamless stratocumulus simulation across the turbulent gray zone. Mon Weather Rev 142:1655–1668. https://doi.org/10.1175/MWR-D-13-00229.1

Chen D, Dai A (2018) Dependence of estimated precipitation frequency and intensity on data resolution. Clim Dyn 50(9):3625–3647. https://doi.org/10.1007/s00382-017-3830-7

Crook J, Klein C, Folwell S, Taylor, Christopher M, Parker DJ, Stein T (2019) Assessment of the representation of West African storm lifecycles in convection-permitting simulations. J Clim. https://doi.org/10.1029/2018EA000491

De Kauwe MG, Taylor CM, Harris PP, Weedon GP, Ellis RJ (2013) Quantifying land surface temperature variability for two Sahelian mesoscale regions during the wet season. J Hydrometeorol 14(5):1605–1619. https://doi.org/10.1175/JHM-D-12-0141.1

Fink AH, Engel T, Ermert V, van der Linden R, Schneidewind M, Redl R, Afiesimama E, Thiaw WM, Yorke C, Evans M, Janicot S (2017) Mean climate and seasonal cycle. In: Parker DJ, Diop-Kane M (eds) Meteorology of tropical West Africa. Wiley-Blackwell, New York, pp 1–39. https://doi.org/10.1002/9781118391297.ch1

Fink AH, Vincent DG, Ermert V (2006) Rainfall types in the West African Sudanian zone during the summer monsoon 2002. Mon Weather Rev 134(8):2143–2164. https://doi.org/10.1175/MWR3182.1

Fiolleau T, Roca R (2013) Composite life cycle of tropical mesoscale convective systems from geostationary and low Earth orbit satellite observations: method and sampling considerations. Q J R Meteorol Soc 139(673):941–953. https://doi.org/10.1002/qj.2174

Fontaine B, Philippon N (2000) Seasonal evolution of boundary layer heat content in the West African monsoon from the NCEP/NCAR reanalysis (1968–1998). Int J Climatol 20:1777–1790. https://doi.org/10.1002/1097-0088(20001130)20:14<1777::AID-JOC568>3.0.CO;2-S

Funk C, Peterson P, Landsfeld M, Pedreros D, Verdin J, Shukla S, Husak G, Rowland J, Harrison L, Hoell A, Michaelsen J (2015a) The climate hazards infrared precipitation with stations: a new environmental record for monitoring extremes. Sci Data 2:150066

Funk C, Verdin A, Michaelsen J, Peterson P, Pedreros D, Husak G (2015) A global satellite-assisted precipitation climatology. Earth Syst Sci Data 7(2):275–287. https://doi.org/10.5194/essd-7-275-2015

Garcia-Carreras L, Marsham JH, Parker DJ, Bain CL, Milton S, Saci A, Salah-Ferroudj M, Ouchene B, Washington R (2013) The impact of convective cold pool outflows on model biases in the Sahara. Geophys Res Lett 40(8):1647–1652. https://doi.org/10.1002/grl.50239

Gehne M, Hamill TM, Kiladis GN, Trenberth KE (2016) Comparison of global precipitation estimates across a range of temporal and spatial scales. J Clim 29(21):7773–7795. https://doi.org/10.1175/JCLI-D-15-0618.1

Hanley KE, Plant RS, Stein THM, Hogan RJ, Nicol JC, Lean HW, Halliwell C, Clark PA (2015) Mixing length controls on high resolution simulations of convective storms. Q J R Meteorol Soc 141(686):272–284. https://doi.org/10.1002/qj.2356

Harris I, Jones PD, Osborn TJ, Lister DH (2014) Updated high-resolution grids of monthly climatic observations—the CRU TS3.10 dataset. Int J Climatol 34:623–642. https://doi.org/10.1002/joc.3711

Hartley AJ, Parker DJ, Garcia-Carreras L, Webster S (2016) Simulation of vegetation feedbacks on local and regional scale precipitation in West Africa. Agric For Meteorol 222:59–70. https://doi.org/10.1016/j.agrformet.2016.03.001

Heinold B, Knippertz P, Marsham JH, Fiedler S, Dixon NS, Schepanski K, Laurent B, Tegen I (2013) The role of deep convection and nocturnal low-level jets for dust emission in summertime West Africa: estimates from convection-permitting simulations. J Geophys Res Atmos 118(10):4385–4400. https://doi.org/10.1002/jgrd.50402

Joyce RJ, Janowiak JE, Arkin PA, Xie P (2004) CMORPH: a method that produces global precipitation estimates from passive microwave and infrared data at high spatial and temporal resolution. J Hydrometeorol 5(3):487–503. https://doi.org/10.1175/1525-7541(2004)005<0487:CAMTPG>2.0.CO;2

Klingaman NP, Martin GM, Moise A (2017) ASoP (v1.0): a set of methods for analyzing scales of precipitation in general circulation models. Geosci Model Dev 10(1):57–83. https://doi.org/10.5194/gmd-10-57-2017

Krishnamurthy PK, Lewis K, Choularton RJ (2014) A methodological framework for rapidly assessing the impacts of climate risk on national-level food security through a vulnerability index. Glob Environ Change 25:121–132. https://doi.org/10.1016/j.gloenvcha.2013.11.004

Laing AG, Carbone R, Levizzani V, Tuttle J (2008) The propagation and diurnal cycles of deep convection in northern tropical Africa. Q J R Meteorol Soc 134(630):93–109. https://doi.org/10.1002/qj.194

Laing AG, Trier SB, Davis CA (2012) Numerical simulation of episodes of organized convection in tropical northern Africa. Mon Weather Rev 140(9):2874–2886. https://doi.org/10.1175/MWR-D-11-00330.1

Leutwyler D, Lüthi D, Ban N, Fuhrer O, Schär C (2017) Evaluation of the convection-resolving climate modeling approach on continental scales. J Geophys Res Atmos. https://doi.org/10.1002/2016JD026013

Liu C, Ikeda K, Rasmussen R, Barlage M, Newman AJ, Prein AF, Chen F, Chen L, Clark M, Dai A, Dudhia J, Eidhammer T, Gochis D, Gutmann E, Kurkute S, Li Y, Thompson G, Yates D

(2016) Continental-scale convection-permitting modeling of the current and future climate of North America. Clim Dyn. https://doi.org/10.1007/s00382-016-3327-9

Lock AP (2001) The numerical representation of entrainment in parameterizations of boundary layer turbulent mixing. Mon Weather Rev 129:1148–1163. https://doi.org/10.1175/1520-0493(2001)129<1148:TNROEI>2.0.CO;2

Maranan M, Fink AH, Knippertz P (2018) Rainfall types over southern West Africa: objective identification, climatology and synoptic environment. Q J R Meteorol Soc. https://doi.org/10.1002/qj.3345

Maraun D, Wetterhall F, Ireson AM, Chandler RE, Kendon EJ, Widmann M, Brienen S, Rust HW, Sauter T, Themessl M, Venema VKC, Chun KP, Goodess CM, Jones RG, Onof C, Vrac M, Thiele-Eich I (2010) Precipitation downscaling under climate change. Recent developments to bridge the gap between dynamical models and the end user. Rev Geophys. https://doi.org/10.1029/2009RG000314

Marsham JH, Knippertz P, Dixon NS, Parker DJ, Lister GM (2011) The importance of the representation of deep convection for modeled dust-generating winds over West Africa during summer. Geophys Res Lett. https://doi.org/10.1029/2011GL048368

Marsham JH, Dixon NS, Garcia-Carreras L, Lister GMS, Parker DJ, Knippertz P, Birch CE (2013) The role of moist convection in the West African monsoon system: insights from continental-scale convection-permitting simulations. Geophys Res Lett 40(9):1843–1849. https://doi.org/10.1002/grl.50347

Martin GM, Klingaman NP, Moise AF (2017) Connecting spatial and temporal scales of tropical precipitation in observations and the MetUM-GA6. Geosci Model Dev 10(1):105–126. https://doi.org/10.5194/gmd-10-105-2017

Mathon V, Laurent H, Lebel T (2002) Mesoscale convective system rainfall in the Sahel. J Appl Meteorol 41(11):1081–1092. https://doi.org/10.1175/1520-0450(2002)041<1081:MCSRIT>2.0.CO;2

Maurer V, Bischoff-Gauß I, Kalthoff N, Gantner L, Roca R, Panitz HJ (2017) Initiation of deep convection in the Sahel in a convection-permitting climate simulation for northern Africa. Q J R Meteorol Soc 143(703):806–816. https://doi.org/10.1002/qj.2966

Meynadier R, Bock O, Gervois S, Guichard F, Redelsperger JL, Agustí-Panareda A, Beljaars A (2010a) West African monsoon water cycle: 2. Assessment of numerical weather prediction water budgets. J Geophys Res Atmos. https://doi.org/10.1029/2010JD013919

Meynadier R, Bock O, Guichard F, Boone A, Roucou P, Redelsperger JL (2010b) West African monsoon water cycle: 1. A hybrid water budget data set. J Geophys Res Atmos. https://doi.org/10.1029/2010JD013917

Mohr KI, Thorncroft CD (2006) Intense convective systems in West Africa and their relationship to the African easterly jet. Q J R Meteorol Soc 132(614):163–176. https://doi.org/10.1256/qj.05.55

Novella NS, Thiaw WM (2013) African rainfall climatology version 2 for famine early warning systems. J Appl Meteorol Climatol 52(3):588–606. https://doi.org/10.1175/JAMC-D-11-0238.1

Parker DJ, Burton RR, Diongue-Niang A, Ellis RJ, Felton M, Taylor CM, Thorncroft CD, Bessemoulin P, Tompkins AM (2005) The diurnal cycle of the West African monsoon circulation. Q J R Meteorol Soc 131(611):2839–2860. https://doi.org/10.1256/qj.04.52

Parker DJ, Kassimou A, Orji BN, Osika DP, Hamza I, Diop-Kane M, Fink A, Galvin J, Guichard F, Lamptey BL, Hamidou H, Linden R, Redl R, Lebel T, Tubbs C (2017) Local weather, chap 4. Wiley-Blackwell, New York, pp 130–174. https://doi.org/10.1002/9781118391297.ch4

Pearson KJ, Hogan RJ, Allan RP, Lister GMS, Holloway CE (2010a) Evaluation of the model representation of the evolution of convective systems using satellite observations of outgoing longwave radiation. J Geophys Res Atmos. https://doi.org/10.1029/2010JD014265

Pearson KJ, Hogan RJ, Allan RP, Lister GMS, Holloway CE (2010b) Evaluation of the model represention of convective systems using satellite observations of outgoing longwave radiation. J Geophys Res. https://doi.org/10.1029/2010JD014265

Pearson KJ, Lister GMS, Birch CE, Allan RP, Hogan RJ, Woolnough SJ (2014) Modelling the diurnal cycle of tropical convection across the "grey zone". Q J R Meteorol Soc 140(679):491–499. https://doi.org/10.1002/qj.2145

Pfeifroth U, Trentmann J, Fink AH, Ahrens B (2016) Evaluating satellite-based diurnal cycles of precipitation in the African tropics. J Appl Meteorol Climatol 55(1):23–39. https://doi.org/10.1175/JAMC-D-15-0065.1

Reynolds RW, Smith TM, Liu C, Chelton DB, Casey KS, Schlax MG (2007) Daily high-resolution blended analyses for sea surface temperature. J Clim 20:5473–5496

Richardson KJ, Lewis KH, Krishnamurthy PK, Kent C, Wiltshire AJ, Hanlon HM (2018) Food security outcomes under a changing climate: impacts of mitigation and adaptation on vulnerability to food insecurity. Clim Change 147(1):327–341. https://doi.org/10.1007/s10584-018-2137-y

Schneider U, Becker A, Finger P, Meyer-Christoffer A, Ziese M, Rudolf B (2014) GPCC's new land surface precipitation climatology based on quality-controlled in situ data and its role in quantifying the global water cycle. Theor Appl Climatol 115:15–40. https://doi.org/10.1007/s00704-013-0860-x

Skamarock WC (2004) Evaluating mesoscale NWP models using kinetic energy spectra. Mon Weather Rev 132(12):3019–3032. https://doi.org/10.1175/MWR2830.1

Smith RNB (1990) A scheme for predicting layer clouds and their water content in a general circulation model. Q J R Meteorol Soc 116:435–460

Stein THM, Hogan RJ, Clark PA, Halliwell CE, Hanley KE, Lean HW, Nicol JC, Plant RS (2015a) The DYMECS project: a statistical approach for the evaluation of convective storms in high-resolution NWP models. Bull Am Meteorol Soc 96:939–951. https://doi.org/10.1175/BAMS-D-13-00279.1

Stein THM, Parker DJ, Hogan RJ, Birch CE, Holloway CE, Lister GMS, Marsham JH, Woolnough SJ (2015b) The representation of the West African monsoon vertical cloud structure in the Met Office Unified Model: an evaluation with CloudSat. Q J R Meteorol Soc 141(693):3312–3324. https://doi.org/10.1002/qj.2614

Stratton RA, Senior CA, Vosper SB, Folwell SS, Boutle IA, Earnshaw D, Kendon E, Lock AP, Malcolm A, Manners J, Morcrette J, Short C, Stirling AJ, Taylor CM, Tucker S, Webster S, Wilkinson JM (2018) A pan-Africa convection-permitting regional climate simulation with the Met Office Unified Model: CP4-Africa. J Clim. https://doi.org/10.1175/JCLI-D-17-0503.1

Taylor CM, Birch CE, Parker DJ, Dixon N, Guichard F, Nikulin G, Lister GMS (2013) Modeling soil moisture-precipitation feedback in the Sahel: importance of spatial scale versus convective parameterization. Geophys Res Lett 40(23):6213–6218. https://doi.org/10.1002/2013GL058511

Trenberth KE, Zhang Y, Gehne M (2017) Intermittency in precipitation: duration, frequency, intensity, and amounts using hourly data. J Hydrometeorol 18(5):1393–1412. https://doi.org/10.1175/JHM-D-16-0263.1

Tropical Rainfall Measuring Mission (TRMM) (2011) TRMM (TMPA) Rainfall Estimate L3 3 h 0.25° × 0.25° V7. Tech. rep., Goddard Earth Sciences Data and Information Services Center (GES DISC), Greenbelt

Vellinga M, Roberts M, Vidale PL, Mizielinski MS, Demory ME, Schiemann R, Strachan J, Bain C (2015) Sahel decadal rainfall variability and the role of model horizontal resolution. Geophys Res Lett. https://doi.org/10.1002/2015GL066690

Vischel T, Quantin G, Lebel T, Viarre J, Gosset M, Cazenave F, Panthou G (2011) Generation of high-resolution rain fields in West Africa: evaluation of dynamic interpolation methods. J Hydrometeorol 12(6):1465–1482. https://doi.org/10.1175/JHM-D-10-05015.1

Vizy EK, Cook KH (2018a) Mesoscale convective systems and nocturnal rainfall over the West African Sahel: role of the Inter-tropical front. Clim Dyn 50(1):587–614. https://doi.org/10.1007/s00382-017-3628-7

Vizy EK, Cook KH (2018b) Understanding the summertime diurnal cycle of precipitation over sub-Saharan West Africa: regions with daytime rainfall peaks in the absence of significant topographic features. Clim Dyn. https://doi.org/10.1007/s00382-018-4315-z

Walters D, Baran A, Boutle I, Brooks M, Earnshaw P, Edwards J, Furtado K, Hill P, Lock A, Manners J, Morcrette C, Mulcahy J, Sanchez C, Smith C, Stratton R, Tennant W, Tomassini L, Van Weverberg K, Vosper S, Willett M, Browse J, Bushell A, Dalvi M, Essery R, Gedney N, Hardiman S, Johnson B, Johnson C, Jones A, Mann G, Milton S, Rumbold H, Sellar A, Ujiie M, Whitall M, Williams K, Zerroukat M (2017) The Met Office Unified Model global atmosphere 7.0/7.1 and JULES global land 7.0 configurations. Geosci Model Dev Discuss 2017:1–78. https://doi.org/10.5194/gmd-2017-291

Wilks DS (2016) "The stippling shows statistically significant grid points": how research results are routinely overstated and overinterpreted, and what to do about it. Bull Am Meteorol Soc 97(12):2263–2273. https://doi.org/10.1175/BAMS-D-15-00267.1

Wilson DR, Bushell AC, Kerr-Munslow AM, Price JD, Morcrette CJ (2008) PC2: a prognostic cloud fraction and condensation scheme. I: scheme description. Q J R Meteorol Soc 134:2093–2107. https://doi.org/10.1002/qj.333

Xie P, Joyce R, Wu S, Yoo SH, Yarosh Y, Sun F, Lin R (2017) Reprocessed, bias-corrected CMORPH global high-resolution precipitation estimates from 1998. J Hydrometeorol 18(6):1617–1641. https://doi.org/10.1175/JHM-D-16-0168.1

Xie P, Chen M, Shi W (2010) CPC unified gauge-based analysis of global daily precipitation. In: Preprints, 24th conference on hydrology, vol 2. Amer. Meteor. Soc., Atlanta

Zhang G, Cook KH (2014) West African monsoon demise: climatology, interannual variations, and relationship to seasonal rainfall. J Geophys Res 119(17):10,175–10,193. https://doi.org/10.1002/2014JD022043

Zhang G, Cook KH, Vizy EK (2016a) The diurnal cycle of warm season rainfall over West Africa. Part I: observational analysis. J Clim 29(23):8423–8437. https://doi.org/10.1175/JCLI-D-15-0874.1

Zhang G, Cook KH, Vizy EK (2016b) The diurnal cycle of warm season rainfall over West Africa. Part II: convection-permitting simulations. J Clim 29(23):8439–8454. https://doi.org/10.1175/JCLI-D-15-0875.1